# Vectorlike fermions and Higgs effective field theory revisited

Chien-Yi Chen, S. Dawson, and Elisabetta Furlan

Phys. Rev. D **96**, 015006 — Published 10 July 2017

DOI: 10.1103/PhysRevD.96.015006

# Vector-like Fermions and Higgs Effective Field Theory Revisited

Chien-Yi Chen
*Department of Physics and Astronomy, University of Victoria, Victoria, BC V8P 5C2, Canada and Perimeter Institute for Theoretical Physics, Waterloo, ON N2J 2W9, Canada*

S. Dawson
*Department of Physics, Brookhaven National Laboratory, Upton, N.Y., 11973 U.S.A.*

Elisabetta Furlan
*Institute for Theoretical Physics, ETH, 8093 Zurich, Switzerland*

(Dated: May 24, 2017)

Heavy vector-like quarks (VLQs) appear in many models of beyond the Standard Model physics. Direct experimental searches require these new quarks to be heavy, $\gtrsim 800-1000$ GeV. We perform a global fit of the parameters of simple VLQ models in minimal representations of $SU(2)_L$ to precision data and Higgs rates. An interesting connection between anomalous $Zb\overline{b}$ interactions and Higgs physics in VLQ models is discussed. Finally, we present our analysis in an effective field theory (EFT) framework and show that the parameters of VLQ models are already highly constrained. Exact and approximate analytical formulas for the $S$ and $T$ parameters in the VLQ models we consider are posted at `https://quark.phy.bnl.gov/Digital_Data_Archive/dawson/vlq_17/` as Mathematica files.

## I. INTRODUCTION

The Standard Model (SM) has been remarkably successful at explaining both precision measurements and LHC data and so the possibilities for heavy, as yet unobserved particles are highly restricted by the experimental results. Here, we focus on new heavy quarks and their impact on electroweak scale physics. Heavy SM-like chiral fermions are excluded by the measured Higgs production rates [1, 2]. Therefore, we consider heavy vector-like quarks (VLQs), which are typically compatible with Higgs measurements. Motivated by the excellent agreement of Higgs measurements with SM predictions [3], we assume that the observed Higgs boson is part of an $SU(2)_L$ doublet, $H$, and consider VLQs which can couple to $H$. This class of VLQs occurs in many composite Higgs models [4–9] and little Higgs models [10–12] and hence is well motivated phenomenologically. The phenomenology of VLQs has been considered in some detail in the literature [13–24] and direct experimental searches [25–38] require them to be heavy, with $M \gtrsim \mathcal{O}(800-1000)$ GeV.

We update previous fits [18–20] to the parameters of VLQ models by performing a joint fit to the oblique parameters and asymmetries in the $b$ quark sector. The study is extended to include restrictions from Higgs coupling measurements with interesting results found in models containing a $B$ VLQ.

We briefly review the set-up of the VLQ models that we study in Section II. Section III reviews the contributions of VLQs to the oblique parameters and the $Zb\overline{b}$ coupling. We find that in some regions of parameter space the leading contributions to the oblique parameters can be quite small even with significant mass splittings between the VLQ multiplet members, due to numerical cancellations. We discuss the effects of these regions on the global fits to VLQ parameters. Section IV contains numerical fits and we present some conclusions in Section V. Appendix A contains a pedagogical description of the triplet models, which should be useful for model builders. The connection between our results in the full VLQ theories and in an EFT approach for heavy VLQ masses is given in Appendix B. Exact and approximate analytical formulas for the oblique parameters in the various models can be found at `https://quark.phy.bnl.gov/Digital_Data_Archive/dawson/vlq_17/`.

## II. VECTOR-LIKE QUARK BASICS

In this section, we introduce our notation for VLQs. We consider the case where the VLQs interact only with the third generation quarks, since mixing with the first two generations is highly restricted by kaon and other low energy physics measurements [16]. We indicate the SM weak eigenstate quarks as,

$$\psi_L^0 = \begin{pmatrix} t_L^0 \\ b_L^0 \end{pmatrix}, \quad t_R^0, b_R^0\,, \tag{2.1}$$

and the Higgs doublet as,

$$H = \begin{pmatrix} \phi^+ \\ \phi^0 \end{pmatrix}\,, \tag{2.2}$$

with $\phi^0 = \frac{v+h}{\sqrt{2}}$. The SM Yukawa couplings are,

$$-L_{Y,SM} = \lambda_t \overline{\psi}_L^0 \tilde{H} t_R^0 + \lambda_b \overline{\psi}_L^0 H b_R^0 + h.c.\,, \tag{2.3}$$

where $\tilde{H} = i\sigma_2 H^*$.

The models we consider have vector-like quarks in the $SU(2)_L$ representations,

$$\begin{aligned}
\text{Singlets}: &\quad T_s^0, \quad B_s^0\,; \\
\text{Doublets}: &\quad \psi_{XT}^0 = (X_d^0, T_d^0), \\
&\quad \psi_{TB}^0 = (T_d^0, B_d^0), \\
&\quad \psi_{BY}^0 = (B_d^0, Y_d^0)\,; \\
\text{Triplets}: &\quad \rho_{XTB}^0 = (X_t^0, T_t^0, B_t^0), \\
&\quad \rho_{TBY}^0 = (T_t^0, B_t^0, Y_t^0)\,.
\end{aligned} \tag{2.4}$$

This is a complete set of VLQ representations that have renormalizable couplings to the SM Higgs doublet. The quarks have electric charge $Q_T = \frac{2}{3}$, $Q_B = -\frac{1}{3}$, $Q_X = \frac{5}{3}$, and $Q_Y = -\frac{4}{3}$. If there is only one VLQ representation, it is simple to write the most general CP conserving couplings between the SM fermions, the VLQs, and the Higgs

boson,[1]

$$
\begin{aligned}
\text{Singlets}: \quad -L_{T_s} &= \lambda_1 \overline{\psi}^0_L \tilde{H} T^0_{(s),R} + M_{T_s} \overline{T}^0_{(s),L} T^0_{(s),R} + h.c. \\
-L_{B_s} &= \lambda_2 \overline{\psi}^0_L H B^0_{(s),R} + M_{B_s} \overline{B}^0_{(s),L} B^0_{(s),R} + h.c. \\
\text{Doublets}: \quad -L_{XT} &= \lambda_3 \overline{\psi}^0_{(XT),L} H t^0_R + M_{XT} \overline{\psi}^0_{(XT),L} \psi^0_{(XT),R} + h.c. \\
-L_{TB} &= \lambda_4 \overline{\psi}^0_{(TB),L} \tilde{H} t^0_R + \lambda_5 \overline{\psi}^0_{(TB),L} H b^0_R + M_{TB} \overline{\psi}^0_{(TB),L} \psi^0_{(TB),R} + h.c. \\
-L_{BY} &= \lambda_6 \overline{\psi}^0_{(BY),L} \tilde{H} b^0_R + M_{BY} \overline{\psi}^0_{(BY),L} \psi^0_{(BY),R} + h.c. \\
\text{Triplets}: \quad -L_{XTB} &= \lambda_7 \bar{\psi}^0_L \sigma^a \rho^{0,a}_{XTB} \tilde{H} + M_{XTB} \bar{\rho}^0_{XTB} \rho^0_{XTB} + h.c. \\
-L_{TBY} &= \lambda_8 \bar{\psi}_L \sigma^a \rho^{0,a}_{TBY} H + M_{TBY} \bar{\rho}^0_{TBY} \rho^0_{TBY} + h.c.
\end{aligned} \tag{2.5}
$$

Note that we do not include mixing between SM fermions and VLQs with identical quantum numbers since these terms can be rotated away by redefinitions of the fields. The singlet and doublet models have been extensively discussed in the literature [13–21], and we include a useful discussion of the details of the triplet model in Appendix A.

The gauge eigenstate fields can be written in general as,

$$
\mathcal{T}^0_{L,R} = \begin{pmatrix} t^0_{L,R} \\ T^0_{L,R} \end{pmatrix} \qquad \mathcal{B}^0_{L,R} = \begin{pmatrix} b^0_{L,R} \\ B^0_{L,R} \end{pmatrix} \tag{2.6}
$$

where $T^0 = T^0_s, T^0_d$ or $T^0_t$ and $B^0 = B^0_s, B^0_d$ or $B^0_t$ (the $X$ and $Y$ fields do not mix with the other fermions and are therefore also mass eigenstates). The terms contributing to the mass matrices are found from Eq. 2.5 and we write them as,

$$
-L_M = \overline{\mathcal{T}}^0_L M^t \mathcal{T}^0_R \; + \overline{\mathcal{B}}^0_L M^b \mathcal{B}^0_R + M_Y \overline{Y}_{t,L} Y_{t,R} + M_X \overline{X}_{t,L} X_{t,R} \, . \tag{2.7}
$$

We denote the mass eigenstate fields as $(t, T)$ and $(b, B)$ and they are found through bi-unitary transformations,

$$
\begin{aligned}
\mathcal{T}_{L,R} &= \begin{pmatrix} t_{L,R} \\ T_{L,R} \end{pmatrix} = V^t_{L,R} \begin{pmatrix} t^0_{L,R} \\ T^0_{L,R} \end{pmatrix} \\
\mathcal{B}_{L,R} &= \begin{pmatrix} b_{L,R} \\ B_{L,R} \end{pmatrix} = V^b_{L,R} \begin{pmatrix} b^0_{L,R} \\ B^0_{L,R} \end{pmatrix} ,
\end{aligned} \tag{2.8}
$$

where

$$
V^{t,b}_{L,R} = \begin{pmatrix} \cos\theta^{t,b}_{L,R} & -\sin\theta^{t,b}_{L,R} \\ \sin\theta^{t,b}_{L,R} & \cos\theta^{t,b}_{L,R} \end{pmatrix} , \tag{2.9}
$$

For simplicity of notation we abbreviate $\cos\theta^t_L \equiv c^t_L$, etc. Through these rotations we obtain the diagonal mass matrices

$$
M^t_{diag} = V^t_L M^t (V^t_R)^\dagger = \begin{pmatrix} m_t & 0 \\ 0 & M_T \end{pmatrix} \quad , \quad M^b_{diag} = V^b_L M^b (V^b_R)^\dagger = \begin{pmatrix} m_b & 0 \\ 0 & M_B \end{pmatrix} . \tag{2.10}
$$

There are relationships between the angles and mass eigenstates that depend on the representation (see for exam-

[1] This can be straightforwardly generalized to models with more than one VLQ representation [20, 21, 39].

| Model | $A^L_{tb}$ | $A^L_{tB}$ | $A^L_{TB}$ | $A^L_{Tb}$ | $A^L_{XT}$ | $A^L_{Xt}$ | $A^L_{BY}$ | $A^L_{bY}$ |
|---|---|---|---|---|---|---|---|---|
| $T_s$ | $c^t_L$ | | | $s^t_L$ | | | | |
| $B_s$ | $c^b_L$ | $s^b_L$ | | | | | | |
| $\psi_{XT}$ | $c^t_L$ | | | $s^t_L$ | $c^t_L$ | $-s^t_L$ | | |
| $\psi_{TB}$ | $c^t_L c^b_L + s^t_L s^b_L$ | $c^t_L s^b_L - s^t_L c^b_L$ | $c^t_L c^b_L + s^t_L s^b_L$ | $s^t_L c^b_L - c^t_L s^b_L$ | | | | |
| $\psi_{BY}$ | $c^b_L$ | $s^b_L$ | | | | | $c^b_L$ | $-s^b_L$ |
| $\psi_{XTB}$ | $c^t_L c^b_L + \sqrt{2} s^t_L s^b_L$ | $c^t_L s^b_L - \sqrt{2} s^t_L c^b_L$ | $s^t_L s^b_L + \sqrt{2} c^t_L c^b_L$ | $s^t_L c^b_L - \sqrt{2} c^t_L s^b_L$ | $\sqrt{2} c^t_L$ | $-\sqrt{2} s^t_L$ | | |
| $\psi_{TBY}$ | $c^t_L c^b_L + \sqrt{2} s^t_L s^b_L$ | $c^t_L s^b_L - \sqrt{2} s^t_L c^b_L$ | $s^t_L s^b_L + \sqrt{2} c^t_L c^b_L$ | $s^t_L c^b_L - \sqrt{2} c^t_L s^b_L$ | | | $\sqrt{2} c^b_L$ | $-\sqrt{2} s^b_L$ |

TABLE I: Left-handed fermion – $W$ couplings as defined in Eq. (2.14). We assume all couplings are real, and neglect the SM CKM angles.

ple [19]),

$$\begin{aligned}
\text{Doublets} \quad (XT): \quad & M_X^2 = M_T^2 (c_R^t)^2 + m_t^2 (s_R^t)^2 \\
(TB): \quad & M_T^2 (c_R^t)^2 + m_t^2 (s_R^t)^2 = M_B^2 (c_R^b)^2 + m_b^2 (s_R^b)^2 \\
(BY): \quad & M_Y^2 = M_B^2 (c_R^b)^2 + m_b^2 (s_R^b)^2 \\
\text{Triplets} \quad (XTB): \quad & M_X^2 = M_T^2 (c_L^t)^2 + m_t^2 (s_L^t)^2 \\
& \qquad = M_B^2 (c_L^b)^2 + m_b^2 (s_L^b)^2 \\
& \sin(2\theta_L^b) = \sqrt{2} \frac{M_T^2 - m_t^2}{(M_B^2 - m_b^2)} \sin(2\theta_L^t) \\
(TBY): \quad & M_Y^2 = M_B^2 (c_L^b)^2 + m_b^2 (s_L^b)^2 \\
& \qquad = M_T^2 (c_L^t)^2 + m_t^2 (s_L^t)^2 \\
& \sin(2\theta_L^b) = \frac{M_T^2 - m_t^2}{\sqrt{2}(M_B^2 - m_b^2)} \sin(2\theta_L^t)
\end{aligned} \tag{2.11}$$

and

$$\begin{aligned}
M_{T,B} \tan\theta_R^{t,b} &= m_{t,b} \tan\theta_L^{t,b} \qquad \text{singlets, triplets} \\
M_{T,B} \tan\theta_L^{t,b} &= m_{t,b} \tan\theta_R^{t,b} \qquad \text{doublets}\,.
\end{aligned} \tag{2.12}$$

Examples of the derivation of these relations are given in Appendix A for the case of vector triplets.

Except for the $(TB)$ doublet model, there are sufficient relationships that the results can always be expressed in terms of two parameters. For our numerical fits, we take as input parameters,

$$\begin{aligned}
B \text{ singlet}: \quad & s_L^b, M_B \\
T \text{ singlet}: \quad & s_L^t, M_T \\
(XT) \text{ doublet}: \quad & s_R^t, M_T \\
(TB) \text{ doublet}: \quad & s_R^t, s_R^b, M_T \\
(BY) \text{ doublet}: \quad & s_R^b, M_B \\
(XTB) \text{ triplet}: \quad & s_L^t, M_T \\
(TBY) \text{ triplet}: \quad & s_L^t, M_T\,.
\end{aligned} \tag{2.13}$$

The couplings to the $W$ boson are,

$$L_W \;=\; \frac{g}{\sqrt{2}} \left( \overline{q}_L^i \gamma_\mu A_{ij}^L q_L^j + \overline{q}_R^i \gamma_\mu A_{ij}^R q_R^j \right) W_\mu^+ + h.c. \tag{2.14}$$

where $q^i, q^j$ are any two quarks in the model for which $Q(q^i) - Q(q^j) = 1$. The values of $A_{ij}^{L,R}$ in the VLQ models we consider are reported in Tabs. I and II.

The neutral current couplings to the $Z$ boson are also modified. The couplings for $f_{i,j} = t, b, T, B, X, Y$ are,

$$\mathcal{L}_Z \;=\; \frac{g}{2c_W} Z_\mu \overline{f}_i \gamma^\mu \left[ X_{ij}^L P_L + X_{ij}^R P_R - 2 Q_i \delta_{ij} s_W^2 \right] f_j\,, \tag{2.15}$$

| Model | $A^R_{tb}$ | $A^R_{tB}$ | $A^R_{TB}$ | $A^R_{Tb}$ | $A^R_{XT}$ | $A^R_{Xt}$ | $A^R_{BY}$ | $A^R_{bY}$ |
|---|---|---|---|---|---|---|---|---|
| $T_s$ | | | | | | | | |
| $B_s$ | | | | | | | | |
| $\psi_{XT}$ | | | | | $c^t_R$ | $-s^t_L$ | | |
| $\psi_{TB}$ | $s^t_R s^b_R$ | $-s^t_R c^b_R$ | $c^t_R c^b_R$ | $-c^t_R s^b_R$ | | | | |
| $\psi_{BY}$ | | | | | | | $c^b_R$ | $-s^b_R$ |
| $\psi_{XTB}$ | $\sqrt{2}s^t_R s^b_R$ | $-\sqrt{2}s^t_R c^b_R$ | $\sqrt{2}c^t_R c^b_R$ | $-\sqrt{2}c^t_R s^b_R$ | $\sqrt{2}c^t_R$ | $-\sqrt{2}s^t_R$ | | |
| $\psi_{TBY}$ | $\sqrt{2}s^t_R s^b_R$ | $-\sqrt{2}s^t_R c^b_R$ | $\sqrt{2}c^t_R c^b_R$ | $-\sqrt{2}c^t_R s^b_R$ | | | $\sqrt{2}c^b_R$ | $-\sqrt{2}s^b_R$ |

TABLE II: Right-handed fermion – $W$ couplings as defined in Eq. (2.14). We assume all couplings are real.

where $s_W = \sin\theta_W$ is the weak mixing angle. The SM couplings are normalized such that $X^L_{ij} = \delta_{ij}$ for $i = t$ and $X^L_{ij} = -\delta_{ij}$ for $i = b$ , with all other $X$ equal to 0. For multiplets containing a heavy charge $-\frac{1}{3}$ quark with isospin $I^B_3$ that mixes with the SM-like $b$ quark or a heavy charge $\frac{2}{3}$ quark with isospin $I^T_3$ that mixes with the SM-like $t$ quark, the diagonal fermion couplings to the $Z$ are[2],

$$X^L_{ii} = I^i_3(1-\delta_{iT})(1-\delta_{iB}) + \delta X^L_{ii} \qquad X^R_{ii} = \delta X^R_{ii}\,, \tag{2.16}$$

where the $I^3_i$ term in the left-handed couplings survive only for the top and bottom quarks, and

$$\begin{array}{lll} \delta X^L_{bb} &=& (s^b_L)^2(I^B_3+1) \\ \delta X^L_{tt} &=& (s^t_L)^2(I^T_3-1) \\ \delta X^L_{BB} &=& -1+(c^b_L)^2(I^B_3+1) \\ \delta X^L_{TT} &=& 1+(c^t_L)^2(I^T_3-1) \\ \delta X^L_{XX} &=& \delta X^R_{XX} = I^X_3 \end{array} \qquad \begin{array}{lll} \delta X^R_{bb} &=& (s^b_R)^2 I^B_3 \\ \delta X^R_{tt} &=& (s^t_R)^2 I^T_3 \\ \delta X^R_{BB} &=& (c^b_R)^2 I^B_3 \\ \delta X^R_{TT} &=& (c^t_R)^2 I^T_3 \\ \delta X^L_{YY} &=& \delta X^R_{YY} = I^Y_3\,. \end{array} \tag{2.17}$$

The off-diagonal couplings to the $Z$ boson are,

$$X^L_{ij} = \delta X^L_{ij}(1-\delta_{ij}) \qquad X^R_{ij} = \delta X^R_{ij}(1-\delta_{ij})\,, \tag{2.18}$$

where

$$\begin{array}{ll} \delta X^L_{bB} &= -s^b_L c^b_L (I^B_3+1) \\ \delta X^L_{tT} &= -s^t_L c^t_L (I^T_3-1) \end{array} \qquad \begin{array}{ll} \delta X^R_{bB} = -s^b_R c^b_R I^B_3 \\ \delta X^R_{tT} = -s^t_R c^t_R I^T_3\,. \end{array} \tag{2.19}$$

Finally, the couplings to the Higgs boson can be parameterized as,

$$L = -\frac{h}{v}\overline{f}^i_L c_{ij} f^j_R + h.c.\,. \tag{2.20}$$

The flavor non-diagonal fermion-Higgs couplings are important for double Higgs production [8, 40] and can be found in Ref. [19]. For models with a singlet or triplet VLQ,

$$c_{ij} = V_L \mathcal{F} V^\dagger_L M_{diag} \tag{2.21}$$

and for models with a doublet VLQ,

$$c_{ij} = M_{diag} V_R \mathcal{F} V^\dagger_R, \tag{2.22}$$

where

$$\mathcal{F} \equiv \begin{pmatrix} 1 & 0 \\ 0 & 0 \end{pmatrix}. \tag{2.23}$$

These formulae hold for both the charge $\frac{2}{3}$ and charge $-\frac{1}{3}$ sectors. The $X$ and $Y$ fermions do not couple to the Higgs. The diagonal Higgs couplings are given in Table III.

[2] $I_3 = (2, 0, -2)$ for triplets, $(1, -1)$ for doublets, 0 for singlets.

| Model | $c_{bb}$ | $c_{BB}$ | $c_{tt}$ | $c_{TT}$ |
|---|---|---|---|---|
| $T_s$ | $m_b$ | - | $m_t(c_L^t)^2$ | $M_T(s_L^t)^2$ |
| $B_s$ | $m_b(c_L^b)^2$ | $M_B(s_L^b)^2$ | $m_t$ | - |
| $\psi_{XT}$ | $m_b$ | - | $m_t(c_R^t)^2$ | $M_T(s_R^t)^2$ |
| $\psi_{TB}$ | $m_b(c_R^b)^2$ | $M_B(s_R^b)^2$ | $m_t(c_R^t)^2$ | $M_T(s_R^t)^2$ |
| $\psi_{BY}$ | $m_b(c_R^b)^2$ | $M_B(s_R^b)^2$ | $m_t$ | - |
| $\psi_{XTB}$ | $m_b(c_L^b)^2$ | $M_B(s_L^b)^2$ | $m_t(c_L^t)^2$ | $M_T(s_L^t)^2$ |
| $\psi_{TBY}$ | $m_b(c_L^b)^2$ | $M_B(s_L^b)^2$ | $m_t(c_L^t)^2$ | $M_T(s_L^t)^2$ |

TABLE III: Diagonal Higgs couplings to fermions.

## III. VLQ CONTRIBUTIONS TO PRECISION MEASUREMENTS

Electroweak precision data place strong restrictions on the parameters of models with VLQs. In this section, we review the contributions to the oblique parameters and the $Zb\overline{b}$ couplings in the VLQ models introduced in the previous section.

### A. Oblique Parameters

The general expression for the contribution to the $T$ parameter from fermions is [4, 13, 41]

$$\begin{aligned} T &= \frac{N_c}{16\pi s_W^2 c_W^2}\sum_{i.j}\Bigg\{\Big(\mid A_{ij}^L\mid^2+\mid A_{ij}^R\mid^2\Big)\theta_+(y_i,y_j)+2\mathrm{Re}\Big(A_{ij}^L A_{ij}^{R*}\Big)\theta_-(y_i,y_j) \\ &\quad -\frac{1}{2}\Bigg[\Big(\mid X_{ij}^L\mid^2+\mid X_{ij}^R\mid^2\Big)\theta_+(y_i,y_j)+2\mathrm{Re}\Big(X_{ij}^L X_{ij}^{R*}\Big)\theta_-(y_i,y_j)\Bigg]\Bigg\}, \end{aligned} \tag{3.1}$$

where $N_c=3$, $y_i\equiv\frac{M_{F_i}^2}{M_Z^2}$, $M_{F_i}$ are the fermion masses, and $A_{ij}^{L,R}$, $X_{ij}^{L,R}$ are defined in Eqs. 2.14 and 2.15 respectively. For the input parameters we use [42] $m_t=173.5$ GeV, $m_b=4.2$ GeV, $m_Z=91.1876$ GeV, $m_W=80.385$ GeV and define the weak angle through $c_W=\frac{m_W}{m_Z}$.
The functions $\theta_\pm(y_i,y_j)$ are,

$$\theta_+(y_1,y_2) = y_1+y_2-\frac{2y_1y_2}{y_1-y_2}\log\left(\frac{y_1}{y_2}\right) \tag{3.2}$$

$$\theta_-(y_1,y_2) = 2\sqrt{y_1y_2}\left[\frac{y_1+y_2}{y_1-y_2}\ln\left(\frac{y_1}{y_2}\right)-2\right]. \tag{3.3}$$

We note that $\theta_+(y,y)=\theta_-(y,y)=0$. When $y_1>>y_2$, $\theta_+(y_1,y_2)\xrightarrow{y_1>>y_2} y_1$ and $\theta_-(y_1,y_2)\xrightarrow{y_1>>y_2}0$. We will make use of these properties as we compute all electroweak parameters in the limit $m_b<<m_t$.

As customary, we subtract the SM top-bottom contribution,

$$\Delta T = T-T_{SM} \tag{3.4}$$

where

$$T_{SM} = \frac{N_c}{16\pi s_W^2 c_W^2}\theta_+(y_t,y_b)=\frac{N_c}{16\pi s_W^2}\frac{m_t^2}{m_W^2}. \tag{3.5}$$

For the top and bottom singlet partner models, the exact results are simple [13, 18]

$$T\text{ singlet}:\ \Delta T^{T_s} = \frac{N_c m_t^2}{16\pi s_W^2 M_W^2}(s_L^t)^2\left[-\left(1+(c_L^t)^2\right)+2(c_L^t)^2\frac{r_T}{r_T-1}\log(r_T)+(s_L^t)^2 r_T\right] \tag{3.6}$$

$$B\text{ singlet}:\ \Delta T^{B_s} = \frac{N_c m_t^2}{16\pi s_W^2 M_W^2}(s_L^b)^2 r_B\left[\frac{2}{1-r_B}\log(r_B)+(s_L^b)^2\right], \tag{3.7}$$

where $r_F \equiv \frac{M_F^2}{m_t^2}$. The contribution to the $T$ parameter in the $(BY)$ doublet model also has a simple expression:

$$(BY)\text{ doublet}: \Delta T^{BY} = -\frac{N_c m_t^2}{128\pi s_W^2 M_W^2} r_B \left\{ 32\frac{(c_R^b)^2}{s_R^b}\log(c_R^b)\left[(c_R^b)^2+1\right] + 8 s_R^b\left[4(c_R^b)^2-(s_R^b)^4\right]\right\}. \tag{3.8}$$

In the large VLQ mass and small mixing angle limits, we obtain simple approximate expressions for the $T$ parameter for all the VLQ representations[3,4]

$$\begin{aligned}
T\text{ singlet}: \quad \Delta T^{T_s} &\sim \frac{N_c m_t^2}{8\pi s_W^2 M_W^2}(s_L^t)^2\left[\log(r_T)-1\right] + \mathcal{O}\left((s_L^t)^4, \frac{1}{r_T}\right)\\
B\text{ singlet}: \quad \Delta T^{B_s} &\sim -\frac{N_c m_t^2}{8\pi s_W^2 M_W^2}(s_L^b)^2\log(r_B) + \mathcal{O}\left((s_L^b)^4, \frac{1}{r_B}\right)\\
(TB)\text{ doublet}: \quad \Delta T^{TB} &\sim \frac{N_c m_t^2 (s_R^t)^2}{8\pi s_W^2 M_W^2}\left[-3+2\log(r_T)\right] + \\
&\qquad \mathcal{O}\left((s_R^t)^4, (s_R^t)^2(s_R^b)^2, (s_R^b)^4, \frac{1}{r_T}\right)\\
(XT)\text{ doublet}: \quad \Delta T^{XT} &\sim \frac{N_c m_t^2 (s_R^t)^2}{8\pi s_W^2 M_W^2}\left[3-2\log(r_T)\right] + \mathcal{O}\left((s_R^t)^4, \frac{1}{r_T}\right)\\
(BY)\text{ doublet}: \quad \Delta T^{BY} &\sim \frac{N_c m_t^2 (s_R^b)^5 r_B}{12\pi s_W^2 M_W^2} + \mathcal{O}\left((s_R^b)^7, \frac{1}{r_B}\right)
\end{aligned}$$

$$\begin{aligned}
(XTB)\text{ triplet}: \quad \Delta T^{XTB} &\sim \frac{N_c m_t^2}{8\pi s_W^2 M_W^2}(s_L^t)^2\left[3\log(r_T)-5\right] + \mathcal{O}\left((s_L^t)^4, \frac{1}{r_T}\right)\\
(TBY)\text{ triplet}: \quad \Delta T^{TBY} &\sim -\frac{N_c m_t^2}{16\pi s_W^2 M_W^2}3(s_L^t)^2\left[\log(r_T)-2\right] + \mathcal{O}\left((s_L^t)^4, \frac{1}{r_T}\right).
\end{aligned} \tag{3.9}$$

The contributions to $\Delta T$ in the various VLQ models are shown in Fig. 1 (Fig. 2 for the $(TB)$ doublet, which has two mixing angles as free parameters). Here we use the exact expressions for the $T$ parameter. For small mixing, the contribution to $\Delta T$ is positive in the $T$ singlet and $(XTB)$ triplet models, negative in the $B$ singlet, $(XT)$ doublet and $(TBY)$ triplet models, and extremely small in the $(BY)$ doublet model (RHS of Fig. 1), as one could expect from the approximate results in Eq. 3.9. In all the models where the $T$ parameter is negative for small mixing $\Delta T$ changes sign at an intermediate value of $\sin\theta$ and therefore vanishes again for non-small mixing. In the case of the $(XT)$ doublet, $\Delta T^{XT} \sim 0$ even for $s_R^t \sim 1$, due to a numerical cancellation. Therefore, in these models there could be regions of parameter space with quite sizeable mixing that are allowed by precision tests. We will explore this possibility in Sec. IV.

The mass splitting between the VLQ multiplet components, $\delta_{Q_1Q_2} \equiv M_{Q_1} - M_{Q_2}$, is fixed by the mixing angles (Eq. 2.11). In the large VLQ mass and small mixing angle approximation, and in the limit for massless bottom quark,

$$\begin{aligned}
\text{Doublets}: \quad \frac{\delta_{TB}}{M_T} &\sim \frac{1}{2}\left[(s_R^t)^2\left(1-\frac{m_t^2}{M_T^2}\right) - (s_R^b)^2\right]\\
\frac{\delta_{XT}}{M_T} &\sim -\frac{(s_R^t)^2}{2}\left(1-\frac{m_t^2}{M_T^2}\right) < 0\\
\frac{\delta_{BY}}{M_B} &\sim \frac{(s_R^t)^2}{2} < \frac{1}{2}
\end{aligned} \tag{3.10}$$

[3] Exact results are posted at `https://quark.phy.bnl.gov/Digital_Data_Archive/dawson/vlq_17/` as a mathematica notebook.

[4] In all our studies we will use the exact expressions for the Peskin-Takeuchi parameters, retaining the full dependence on the VLQs masses and on the mixing angles.

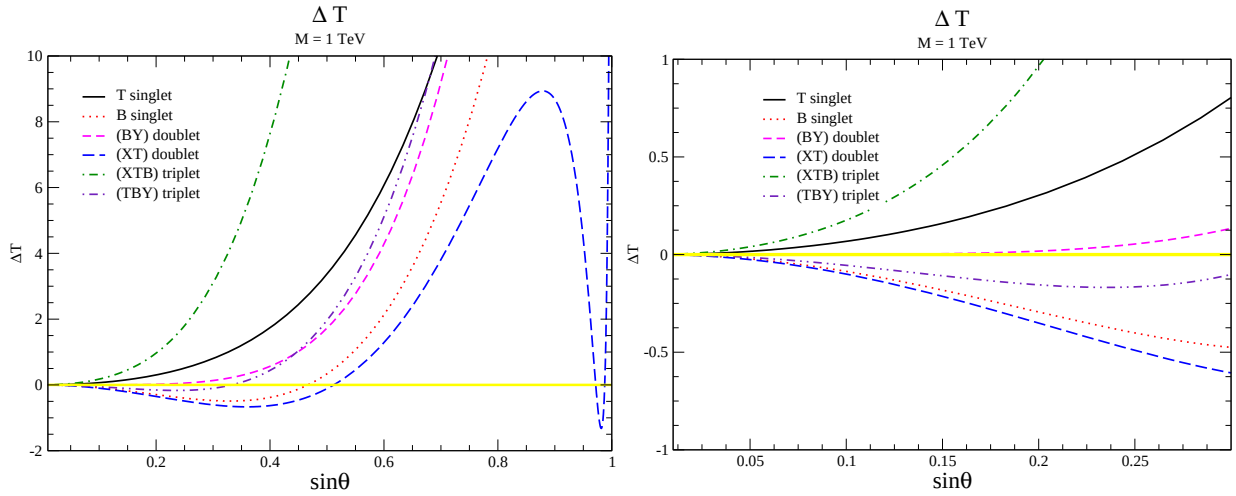


FIG. 1: Exact results for $\Delta T$ for $M = 1$ TeV in the VLQ models. $\sin\theta$ and $M$ are identified in Eq. 2.13.

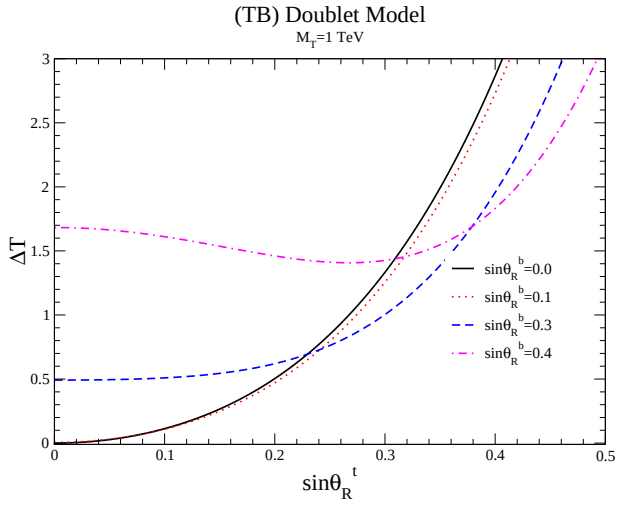


FIG. 2: Exact results for $\Delta T$ for $M_T = 1$ TeV in the $(TB)$ doublet model.

$$\text{Triplets}: \quad \begin{aligned} \frac{\delta_{TB}}{M_T} &\sim \frac{1}{2}\left[(s_L^t)^2\left(1-\frac{m_t^2}{M_T^2}\right)-(s_L^b)^2\right] \\ \frac{\delta_{XT}}{M_T} &\sim -\frac{(s_L^t)^2}{2}\left(1-\frac{m_t^2}{M_T^2}\right) < 0 \\ \frac{\delta_{BY}}{M_B} &\sim \frac{(s_L^b)^2}{2} < \frac{1}{2}\,. \end{aligned} \tag{3.11}$$

From Eq. 3.11, in all cases $\frac{\delta}{M} \sim \sin^2\theta_i$, so for small angles $\Delta T$ grows with the mixing between the SM fermions and the VLQs. For large masses, the mixing goes to zero for fixed Yukawa couplings (see Table III), and decoupling is recovered [18].

The expression for the contributions to the $S$ parameter from fermions is [13, 41, 43]

$$\begin{aligned} S \;=\; \frac{N_c}{2\pi}\sum_{i,j}\Bigg\{ &\left(\mid A_{ij}^L\mid^2+\mid A_{ij}^R\mid^2\right)\psi_+(y_i,y_j)+2\mathrm{Re}\left(A_{ij}^L A_{ij}^{R*}\right)\psi_-(y_i,y_j) \\ &-\frac{1}{2}\left[\left(\mid X_{ij}^L\mid^2+\mid X_{ij}^R\mid^2\right)\chi_+(y_i,y_j)+2\mathrm{Re}\left(X_{ij}^L X_{ij}^{R*}\right)\chi_-(y_i,y_j)\right]\Bigg\}, \end{aligned} \tag{3.12}$$

where we subtract the SM top-bottom contribution,

$$\Delta S = S - S_{SM} \tag{3.13}$$

$$S_{SM} = \frac{N_c}{6\pi}\left[1 - \frac{1}{3}\log\left(\frac{m_t^2}{m_b^2}\right)\right]. \tag{3.14}$$

The functions appearing in $S$ are [13],

$$\begin{aligned}
\psi_+(y_1,y_2) &= \frac{1}{3} - \frac{1}{9}\log\frac{y_1}{y_2} \\
\psi_-(y_1,y_2) &= -\frac{y_1+y_2}{6\sqrt{y_1 y_2}} \\
\chi_+(y_1,y_2) &= \frac{5(y_1^2+y_2^2)-22y_1y_2}{9(y_1-y_2)^2} + \frac{3y_1y_2(y_1+y_2)-y_1^3-y_2^3}{3(y_1-y_2)^3}\log\frac{y_1}{y_2} \\
\chi_-(y_1,y_2) &= -\sqrt{y_1y_2}\left[\frac{y_1+y_2}{6y_1y_2} - \frac{y_1+y_2}{(y_1-y_2)^2} + \frac{2y_1y_2}{(y_1-y_2)^3}\log\frac{y_1}{y_2}\right]
\end{aligned} \tag{3.15}$$

where $\chi_+(y,y) = \chi_-(y,y) = 0$ and in the limit $y_1 >> y_2$,

$$\begin{aligned}
\psi_+(y_1,y_2) &\xrightarrow{y_1>>y_2} \tfrac{1}{3} - \tfrac{1}{9}\log\left(\tfrac{y_1}{y_2}\right), \;\; \psi_-(y_1,y_2) \xrightarrow{y_1>>y_2} -\frac{1}{6}\sqrt{\frac{y_1}{y_2}} \\
\chi_+(y_1,y_2) &\xrightarrow{y_1>>y_2} \tfrac{5}{9} - \tfrac{1}{3}\log\left(\tfrac{y_1}{y_2}\right), \;\; \chi_-(y_1,y_2) \xrightarrow{y_1>>y_2} -\frac{1}{6}\sqrt{\frac{y_1}{y_2}}
\end{aligned} \tag{3.16}$$

For the singlet bottom and top VLQ models, the exact results (full mass and angle dependence) are

$$\begin{aligned}
T \text{ singlet}: \;\; \Delta S^{T_s} = \; & -\frac{N_c}{18\pi}(s_L^t)^2\left[\log(r_T) + (c_L^t)^2\left(\frac{5(r_T^2+1)-22r_T}{(r_T-1)^2}\right.\right. \\
& \left.\left. + \frac{3(r_T+1)(r_T^2-4r_T+1)}{(1-r_T)^3}\log(r_T)\right)\right],
\end{aligned} \tag{3.17}$$

$$B \text{ singlet}: \;\; \Delta S^{B_s} = \frac{N_c}{18\pi}(s_L^b)^2\left[-5(c_L^b)^2 + \left(4 - 3(s_L^b)^2\right)\log\frac{r_B}{r_b}\right]. \tag{3.18}$$

As in the case of the $T$ parameter, the $(BY)$ doublet model also has a simple exact expression for $S$,

$$(BY) \text{ doublet}: \;\; \Delta S^{BY} = \frac{N_c}{18\pi}\left\{4(c_R^b)^2\log(c_R^b) + (s_R^b)^2\left[1 + 5(s_R^b)^2 + \left(2 - 3(s_R^b)^2\right)\log\frac{r_B}{r_b}\right]\right\}. \tag{3.19}$$

The contributions to $\Delta S$ are shown in Figs. 3 and 4 using the exact results (full mass and angle dependence) in all the models.

In the heavy VLQ mass limit (and assuming small mixings between the doublet and triplet components),[5]

$$\begin{aligned}
T \text{ singlet}: \;\; \Delta S^{T_s} &\sim \frac{N_c}{18\pi}(s_L^t)^2\left[-5 + 2\log(r_T)\right] + \mathcal{O}\left((s_L^t)^4, \frac{1}{r_T}\right) \\
B \text{ singlet}: \;\; \Delta S^{B_s} &\sim \frac{N_c}{18\pi}(s_L^b)^2\left[-5 + 4\log\frac{r_B}{r_b}\right] + \mathcal{O}\left((s_L^b)^4, \frac{1}{r_B}\right)
\end{aligned}$$

[5] Exact results are posted at `https://quark.phy.bnl.gov/Digital_Data_Archive/dawson/vlq_17/` as a mathematica notebook.

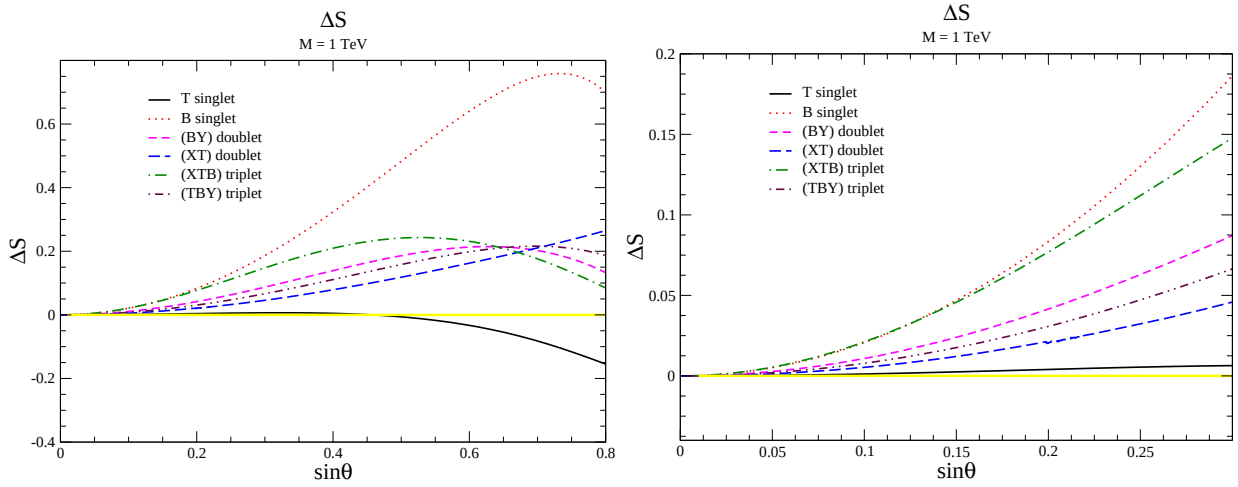


FIG. 3: Exact results for $\Delta S$ for $M = 1$ TeV in the VLQ models. The parameters $\sin\theta$ and $M$ are identified in Eq. 2.13.

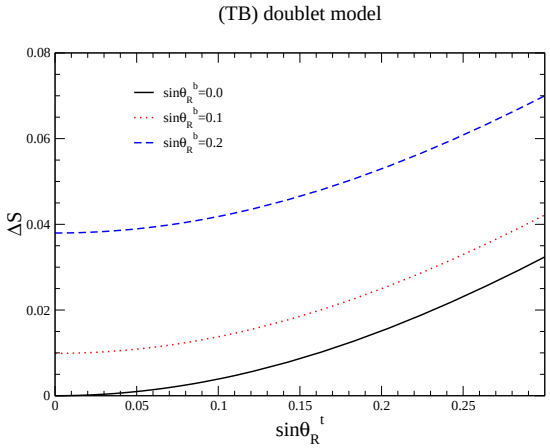


FIG. 4: Exact results for $\Delta S$ for $M = 1$ TeV in the $(TB)$ doublet model.

$$
\begin{aligned}
(TB)\text{ doublet}: \quad \Delta S^{TB} \sim\ & -\frac{N_c}{18\pi}\left\{(s_R^b)^2\left[3+2\log\left(\frac{r_b}{r_T}\right)\right]+(s_R^t)^2\left[7-4\log(r_T)\right]\right\}+ \\
& \mathcal{O}\left((s_R^t)^4,(s_R^t)^2(s_R^b)^2,(s_R^b)^4,\frac{1}{r_T}\right) \\
(XT)\text{ doublet}: \quad \Delta S^{XT} \sim\ & \frac{N_c}{18\pi}(s_R^t)^2\left[3+2\log(r_T)\right]+\mathcal{O}\left((s_R^t)^4,\frac{1}{r_T}\right) \\
(BY)\text{ doublet}: \quad \Delta S^{BY} \sim\ & \frac{N_c(s_R^b)^2}{18\pi}\left[-1+2\log\left(\frac{r_B}{r_b}\right)\right]+\mathcal{O}\left((s_R^b)^4,\frac{1}{r_B}\right) \\
(XTB)\text{ triplet}: \quad \Delta S^{XTB} \sim\ & -\frac{N_c}{18\pi}(s_L^t)^2\left[7+4\log(r_b)-6\log(r_T)\right]+\mathcal{O}\left((s_L^t)^4,\frac{1}{r_T}\right) \\
(TBY)\text{ triplet}: \quad \Delta S^{TBY} \sim\ & \frac{N_c}{36\pi}(s_L^t)^2\left[1+8\log(r_T)\right]+\mathcal{O}\left((s_L^t)^4,\frac{1}{r_T}\right). \qquad (3.20)
\end{aligned}
$$

The $B$ singlet, $(XT)$ doublet, and $(TBY)$ triplet models have the interesting feature that $\Delta T$ vanishes for particular fine-tuned choices of the parameters with non-zero mass splittings between the members of the VLQ multiplets. In the left panel of Fig. 5 we show the VLQ mass and mixing angle for which $\Delta T = 0$ and in the right panel we show $\Delta S$ for these parameters.

The oblique fit, ignoring correlations, requires $\Delta S < 0.3$ at 95 % confidence level [44, 45], so there are regions where both $\Delta T$ and $\Delta S$ can escape the oblique constraints in these models. These fined-tuned regions will have

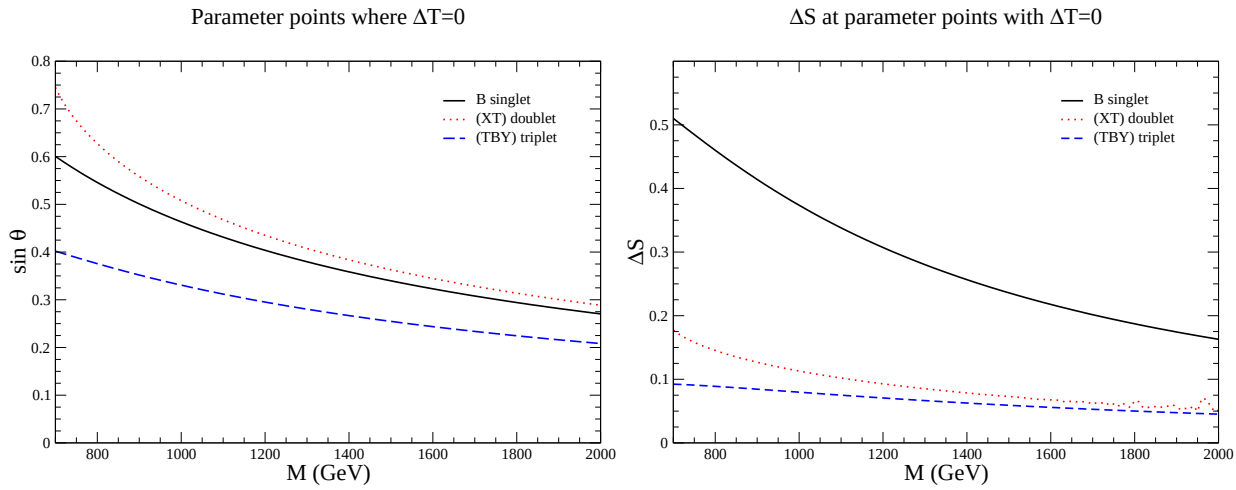


FIG. 5: Left panel: fine-tuned parameter points where $\Delta T = 0$ in the $B$ singlet, $(XT)$ doublet and $(TBY)$ triplet models. The parameters $\sin\theta$ and $M$ are identified in Eq. 2.13. Right panel: values of the $S$ parameter corresponding to the points on the LHS.

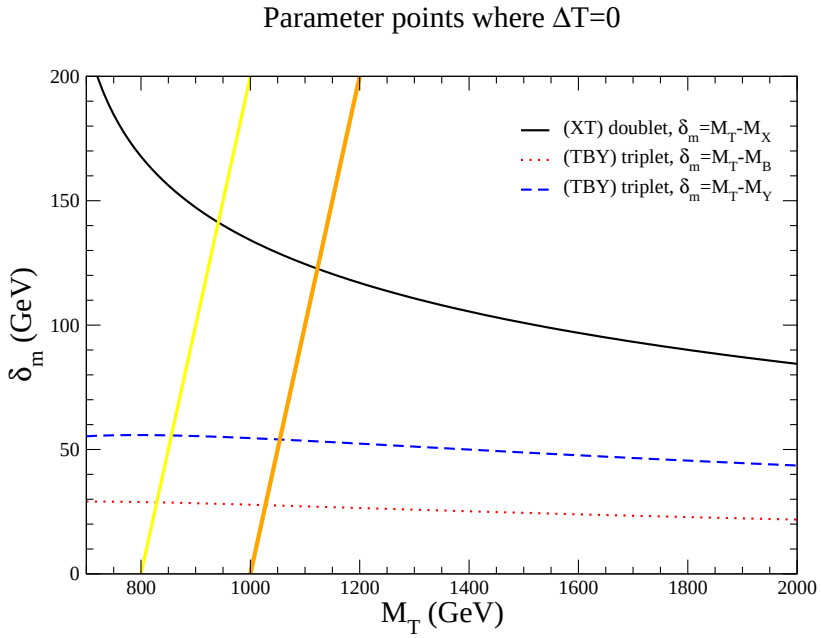


FIG. 6: VLQ multiplet mass splittings for parameter points where $\Delta T = 0$. Below and to the right of the yellow (orange) line, all VLQs have masses larger than 800 GeV (1 TeV).

important impacts on the global fits in the next section and we note that the mass splittings between VLQ multiplet members can be significant for these choices of parameters. Fig. 6 shows the mass difference for the points where $\Delta T$ is fine-tuned to be zero, corresponding to the mixing angles of Fig. 5.

### B. Contributions to $Zb\bar{b}$

In the VLQ models where $\delta X^L_{bb}$ vanishes at tree level, we will use the one-loop contributions to the left-handed $Zb\bar{b}$ coupling for our fit to electroweak precision data. This occurs in the $(TB)$ doublet model (Eq. 2.17), as well as in the

$T$ singlet and $(XT)$ doublet models. The one-loop corrections from $t-T$ mixing to $\delta X_{bb}^L$ are [4, 14],

$$\delta X_{bb}^L = \frac{g^2}{32\pi^2}(s_L)^2\left(f_1(x,x') + (c_L^t)^2 f_2(x,x')\right), \tag{3.21}$$

where $x = m_t^2/M_W^2$, $x' = M_T^2/M_W^2$ and the SM contribution has been subtracted. In the limit $x, x' >> 1$,

$$\begin{aligned} f_1(x,x') &= x' - x + 3\log\left(\frac{x'}{x}\right) \\ f_2(x,x') &= -x - x' + \frac{2xx'}{x'-x}\log\left(\frac{x'}{x}\right). \end{aligned} \tag{3.22}$$

## IV. NUMERICAL RESTRICTIONS ON VLQS

The properties of VLQ models are restricted by $Zb\overline{b}$, oblique parameter, and Higgs coupling measurements. In this section, we perform global fits to $Zb\overline{b}$ and oblique parameter data and demonstrate that Higgs coupling measurements are not competitive with the limits from the electroweak parameters.

The experimental constraints from the right-handed $Zb\overline{b}$ coupling are considerably weaker than those from the left-handed coupling, so we consider only right-handed couplings, $\delta X_{bb}^R$, that arise at tree level. On the other hand, if the left-handed coupling is zero at tree level, we include the loop corrections from $t-T$ mixing using the $1-$loop results of Refs. [4, 14] reported in Eq. 3.21. In the VLQ models where $\delta X_{bb}^R = 0$ at tree level, ($T$ and $B$ singlet, $(XT)$ doublet, $(TBY)$ triplet), we use the $3-$parameter fit to $\Delta S$, $\Delta T$ and $\delta X_{bb}^L$ from Ref. [44][6]. In addition, $\delta X_{bb}^R \sim 0$ at tree level also in the $(XTB)$ triplet model in the limit $m_b << M_B$ (Eq. 2.12), and it vanishes in the $(TB)$ doublet model when we fix $s_R^b = 0$. In all these cases we use the $3-$parameter fit,

$$\begin{aligned} \Delta S &= 0.10 \pm 0.09 \\ \Delta T &= 0.12 \pm 0.07 \\ \delta X_{bb}^L &= -0.0002 \pm 0.0012 \end{aligned} \tag{4.1}$$

with the correlation matrix,

$$\rho = \begin{pmatrix} 1.0 & 0.85 & 0.07 \\ 0.85 & 1.0 & 0.13 \\ 0.07 & 0.13 & 1.0 \end{pmatrix}. \tag{4.2}$$

In the $(BY)$ model we have non-zero values for $\Delta S$, $\Delta T$ and $\delta X_{bb}^R$. In the small bottom-mass limit $\delta X_{bb}^L$ will be extremely suppressed and one can neglect it. Indeed, for $m_b \to 0$ the left-handed $Zb\bar{b}$ coupling is zero at tree level. The one-loop contributions vanish as well, since all the electroweak couplings of the bottom quark are proportional to $s_L^b$, which in this limit goes to zero (Eq. 2.12). The $3-$parameter fit we use in this case is,

$$\begin{aligned} \Delta S &= 0.08 \pm 0.09 \\ \Delta T &= 0.10 \pm 0.07 \\ \delta X_{bb}^R &= 0.008 \pm 0.006 \end{aligned} \tag{4.3}$$

with the correlation matrix,

$$\rho = \begin{pmatrix} 1.0 & 0.86 & -0.19 \\ 0.86 & 1.0 & -0.21 \\ -0.19 & -0.21 & 1.0 \end{pmatrix}. \tag{4.4}$$

When both $\delta X_{bb}^L$ and $\delta X_{bb}^R$ are non-zero, we use the $4-$parameter fit of Ref. [44] to $\Delta S$, $\Delta T$, $\delta X_{bb}^R$ and $\delta X_{bb}^L$. For a massless $b$ quark, this case only occurs in the $(TB)$ doublet model, where $\delta X_{bb}^L$ arises at one loop. The $4-$parameter

[6] $\delta X_{bb}^L = 2\delta g_L^b$ in the notation of Ref. [44].

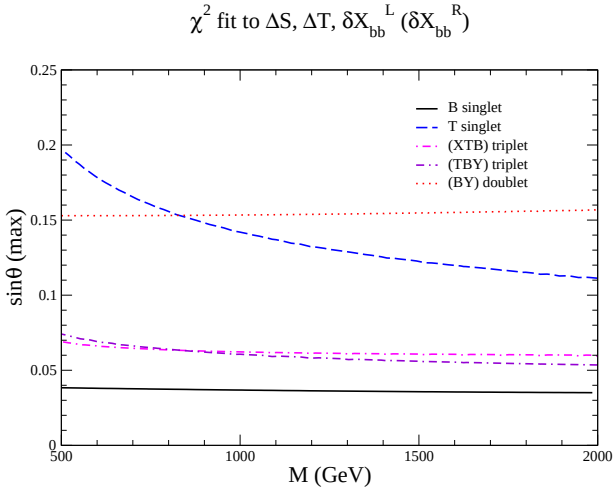


FIG. 7: 95% confidence level allowed regions in the various VLQ models models, where the meanings of $\sin\theta$ and $M$ are defined in Eq. 2.13. The regions below the curves are allowed.

fit is,

$$\begin{aligned} \Delta S &= 0.04 \pm 0.09 \\ \Delta T &= 0.08 \pm 0.07 \\ \delta X_{bb}^L &= 0.006 \pm 0.002 \\ \delta X_{bb}^R &= 0.034 \pm 0.016 \end{aligned} \tag{4.5}$$

with the correlation matrix,

$$\rho = \begin{pmatrix} 1.0 & 0.86 & -0.24 & -0.29 \\ 0.86 & 1.0 & -0.15 & -0.22 \\ -0.24 & -0.15 & 1.0 & 0.91 \\ -0.29 & -0.22 & 0.92 & 1.0 \end{pmatrix} . \tag{4.6}$$

We perform a $\chi^2$ fit,

$$\Delta\chi^2 = \Sigma_{ij}(O_i - O_i^{fit})(\sigma^2)_{ij}^{-1}(O_j - O_j^{fit}) , \tag{4.7}$$

where $O_i$ are the measured observables ($\Delta S$, $\Delta T$, $\delta X_{bb}^L$, $\delta X_{bb}^R$), $O_i^{fit}$ are their predicted values in the different VLQ models, and $\sigma_{ij}^2 = \sigma_i \rho_{ij} \sigma_j$, where $\sigma_i$ are the uncertainties in Eqs. 4.1, 4.3 and 4.5. The correlation matrices are given in Eqs. 4.2, 4.4 and 4.6. In each model, we scan over the parameters to obtain the 95% confidence level limits. All the models but the $(TB)$ doublet have two independent degrees of freedom (see Eq. 2.13). Also in the $(TB)$ model we will analyse two specific scenarios, one with $s_R^b$ fixed, and one with $M_T$ fixed. Therefore, in all cases the number of degrees of freedom is two, and we require $\Delta\chi^2 < 5.99$.

Our results for the regions of parameter space allowed by the electroweak precision observables are shown in Figs. 7, 8 and 9, where we use the exact results for the oblique parameters[7].

Ref. [19] showed limits from the oblique parameters and the $Zb\bar{b}$ couplings separately, and our fit results are roughly consistent with theirs, although the experimental constraints have tightened somewhat. For the $T$, $B$ singlet models, the $(BY)$ doublet model and the triplet models, the limits on the mixing angles are quite stringent and for large VLQ masses relatively independent of the VLQ mass itself (Fig. 7).

The $(XT)$ doublet model has an interesting region seen in Fig. 8 (black dotted area), where the contribution to $\Delta T$ vanishes, allowing relatively large values of the mixing angle. This region is consistent with the $\Delta T \sim 0$ region of

[7] The exact result for $\Delta S$ in the $(XT)$ doublet model shows numerical instabilities in the small angle region. Hence, we have used an expansion up to $\mathcal{O}\left((s_R^t)^{16}\right)$ for $s_R^t < 0.2$. At the matching point, the exact result is stable and the difference with the expanded one is below the percent level.

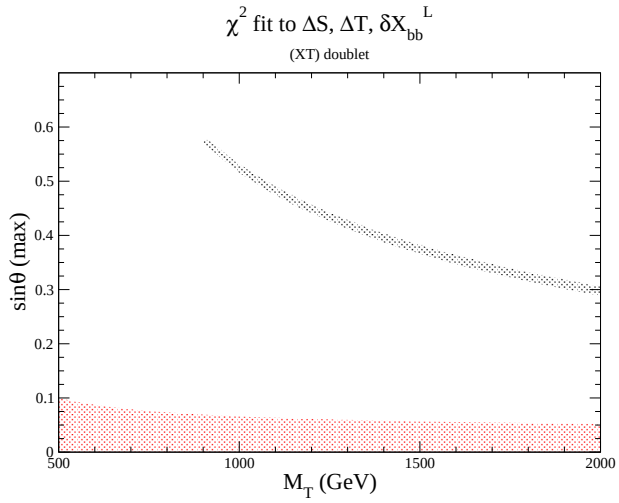


FIG. 8: 95% confidence level allowed regions in the $(XT)$ doublet model, where the dotted regions are allowed.

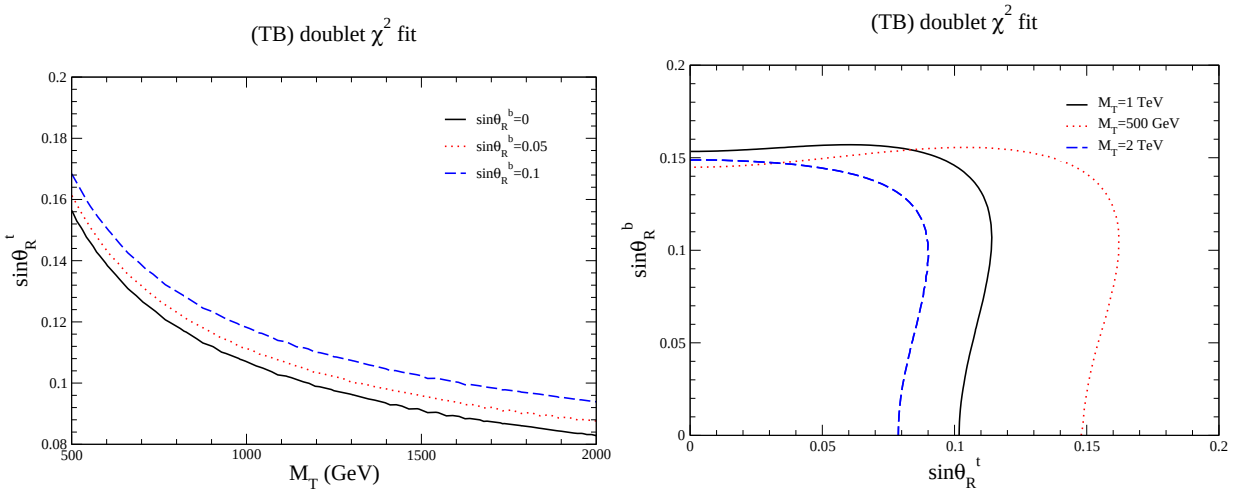


FIG. 9: 95% confidence level allowed regions in the $(TB)$ doublet model for different, fixed values of $s_R^b$ (LHS) and $M_T$ (RHS). The regions below the curves are allowed. The fits in the two panels are performed separately, setting $s_R^b$ (LHS) and $M_T$ (RHS) to a fixed value and fitting to the other two independent parameters represented on the $x$ and $y$ axis. The minimum chi-square of the fits are different in the two panels.

Fig. 1 for $M_T = 1$ TeV.

Also in the $(TB)$ doublet model (Fig. 9) we find an interesting region with non-zero mixings both in the top and bottom sectors allowed by the fit. On the RHS of Fig. 9, we see the allowed region when both $s_R^t$ and $s_R^b$ are non-zero for fixed VLQ mass. The maximum value of $s_R^b \sim 0.15$ is relatively independent of $M_T$, while the maximum value of $s_R^t$ decreases with increasing VLQ mass. On the LHS of Fig. 9, the dependence of the maximum value of $s_R^t$ on $s_R^b$ can be seen to be very slight, for fixed $M_T$. Doing a global fit strengthens the bounds in the $(TB)$ and $(XTB)$ models relative to those of Ref. [19]. Models with $B$ VLQs [46] are allowed by the fits, with a relatively large mixing angle permitted in the $(BY)$ doublet model. The strongest limit on models with $B$ VLQs occurs in the $B$ singlet case, where for all $M_B$, the global fit requires $s_L^b < 0.04$ due to the strong dependence of $\delta X_{bb}^L$ on the mixing angle (Eq. 2.17). We note that for large VLQ masses, the fits asymptote to an approximately constant mixing angle in each case. This suggests that the value of the VLQ mass is not critical and that an effective field theory (EFT) approach is warranted. We discuss the EFT approach for heavy VLQs in Appendix B.

We have presented our results in terms of the masses and mixing angles given in Eq. 2.13. Using Eq. 3.11, we redisplay our fit results in terms of the allowed mass differences between members of the VLQ multiplets. In Fig. 10, we demonstrate that the maximum allowed mass differences are of $\mathcal{O}(1-3$ GeV), except for the $(BY)$ and $(TB)$ doublet models. For $M \sim 1$ TeV, the maximum allowed mass splitting for the $(BY)$ model is $\sim 10$ GeV, increasing

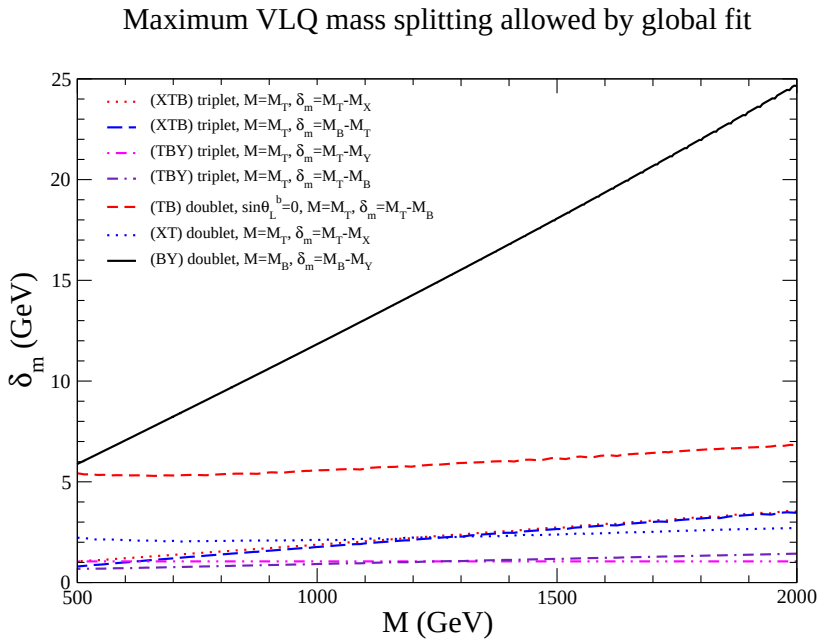


FIG. 10: Maximum allowed mass splitting between the members of a VLQ multiplet using the results of Fig. 7.

to $\sim 25$ GeV for $M \sim 2$ TeV. For the $(TB)$ model, the maximum mass splitting is $\sim 5$ GeV, independent of the VLQ masses.

The mixing of SM and vector-like quarks changes the $tbW$ couplings, $A_{tb}^{L,R}$. The limits from 7 and 8 TeV data from $t-$channel single top production [19, 47] are however not yet competitive with the precision electroweak limits. Limits on the mixing angles in VLQ models can also be determined from direct searches for single production of a heavy VLQ. These limits are model dependent, but tend to be weaker than those from our precision electroweak fits, especially as $M$ is increased. For example, in the $T$ singlet model the search for single $T$ production in the $T \to Wb$ channel requires $s_R^t < 0.32$ (0.69) for $M_T = 1$ (1.5) TeV [38]. In the $(BY)$ doublet model, the same analysis requires $s_R^t < 0.23$ (0.56) for $M_T = 1(1.5)$ TeV.

Finally, in the VLQ models Higgs production and decay rates are modified. The Higgs signal strengths for the gluon fusion production channel using the 95% confidence level results at 8 TeV are [3],

$$\begin{aligned} \mu_F^{\gamma\gamma} &= 1.13^{+0.24}_{-0.21} \\ \mu_F^{WW} &= 1.08^{+0.22}_{-0.19} \\ \mu_F^{ZZ} &= 1.29^{+0.29}_{-0.25} \\ \mu_F^{bb} &= 0.65^{+0.37}_{-0.28} \\ \mu_F^{\tau\tau} &= 1.07^{+0.35}_{-0.28}\,. \end{aligned} \tag{4.8}$$

The production rate $gg \to h$ and the decays $h \to gg$ and $h \to \gamma\gamma$ are affected by the VLQ contributions through loops of heavy quarks and changes in the SM quarks Yukawa couplings, while the $h \to b\bar{b}$ decay is modified at tree level.

The contribution to the Higgs signal strength from colored fermions is well known. At leading order [48],

$$\mu_{ggF} \equiv \frac{\sigma(gg \to h)}{\sigma(gg \to h)\,|_{SM}} = \frac{|\sum_{f=t,b,T,B} \frac{c_{ff}}{m_f} F_F(\tau_f)\,|^2}{|\sum_{f=t,b} \frac{c_{ff}^{SM}}{m_f} F_F(\tau_f)\,|^2}\,, \tag{4.9}$$

where $c_{ff}$ are the Higgs-fermion couplings defined in Eq. 2.20, $m_f$ is the mass of the corresponding quark, $c_{ff}^{SM} = m_f$,

$\tau_f = \frac{m_h^2}{4M_f^2}$, and

$$\begin{aligned} F_F(x) &= \frac{2}{x^2}\Big[x + (x-1)f(x)\Big] \\ f(x) &= \begin{cases} \Big[\sin^{-1}(\sqrt{x})\Big]^2 & x < 1 \\ -\frac{1}{4}\Big[\ln(x_+/x_-) - i\pi\Big]^2 & x > 1 \end{cases} \\ x_\pm &= 1 \pm \sqrt{1 - \frac{1}{x}}\,. \end{aligned} \tag{4.10}$$

In the heavy fermion mass limit $F_F(x) \to \frac{4}{3}$, while for light quarks $F_F(\tau_b) \to 0$. Therefore in the limit of massless $b$ quark and infinitely heavy $(t, T, B)$ quarks, the leading order Higgs production rate is independent of the fermion masses,

$$\mu_{ggF} = \frac{\sigma(gg \to h)}{\sigma(gg \to h)\,|_{SM}} \to |\,\Sigma_{f=(t,T,B)} \frac{c_{ff}}{m_f}\,|^2\ . \tag{4.11}$$

The deviations of the gluon fusion production rate, $\mu_{ggF}$, are directly related to deviations in the $b$ couplings,

$$\begin{aligned} T, (XT):&\ \mu_{ggF} \to\ 1 \\ B, (TBY):&\ \mu_{ggF} \to\ 1 + 2(s_L^b)^2 = 1 + \delta X_{bb}^L \\ (XTB):&\ \mu_{ggF} \to\ 1 + 2(s_L^b)^2 = 1 - \delta X_{bb}^L \\ (TB):&\ \mu_{ggF} \to\ 1 + 2(s_R^b)^2 = 1 - \delta X_{bb}^R \\ (BY):&\ \mu_{ggF} \to\ 1 + 2(s_R^b)^2 = 1 + \delta X_{bb}^R\,. \end{aligned} \tag{4.12}$$

We observe that in all cases the presence of heavy $B$ VLQs *increases* the Higgs signal strength.

For the decay width to photons we have,

$$\begin{aligned} \mu^{\gamma\gamma} &\equiv \frac{\Gamma(h \to \gamma\gamma)}{\Gamma(h \to \gamma\gamma)\,|_{SM}} \\ &= \frac{|\,\Sigma_{f=f_{SM},T,B} N_c Q_f^2 (c_{ff}/m_f) F_F(\tau_f) + F_W(\tau_W)\,|^2}{|\,\Sigma_{f=f_{SM}} N_c Q_f^2 F_F(\tau_f) + F_W(\tau_W)\,|^2}\,, \end{aligned} \tag{4.13}$$

where $f_{SM}$ includes all SM fermions, $Q_f$ and $N_c$ are charge and color of the fermion, $F_F(x)$ is defined in Eq. 4.10 and

$$\begin{aligned} F_W(x) &= -\frac{1}{x^2}\Big[2x^2 + 3x + 3(2x-1)f(x)\Big] \qquad , \quad \text{with} \\ F_W(0) &\to -7\,. \end{aligned} \tag{4.14}$$

Modifications of Higgs signal strength for the various VLQs are shown in Figs. 11, 12, 13 and 14, where we define,

$$\mu_{ggF}^{XX} \equiv \frac{\sigma(gg \to h) BR(h \to XX)}{[\sigma(gg \to h) BR(h \to XX)]_{SM}}\,. \tag{4.15}$$

The $B$ and $T$ singlet and $XT$ doublet models are so highly constrained by the electroweak fits, that the deviations in Higgs production are too small to be observed. In the $(XT)$ doublet model, there is a fine-tuned region (around $s_R^t \sim 0.5$ for $M_T \sim 1$ TeV) where $\Delta T = 0$. In this region, the $\gamma\gamma$ signal strength is reduced by $\sim 1$ %, while the $WW, ZZ$ and $bb$ signal strengths are reduced by $\sim$ 2%. In the $(BY)$ model, the shift in the gluon fusion $WW$ and $ZZ$ signal strengths can be $\sim 10$ % for the maximum allowed mixing, $s_R^b \sim 0.15$, while the increase in the $bb$ signal strength can be as large as $\sim 7$ % (see Fig. 12). The $(TB)$ doublet model can have modest increases in Higgs signal strengths when the mixing in the right-handed $b$ sector is allowed to be significant (RHS of Fig. 13). In the $(XTB)$ triplet triplet model, the Higgs decay channels are constrained to be within about 4% of the SM predictions.

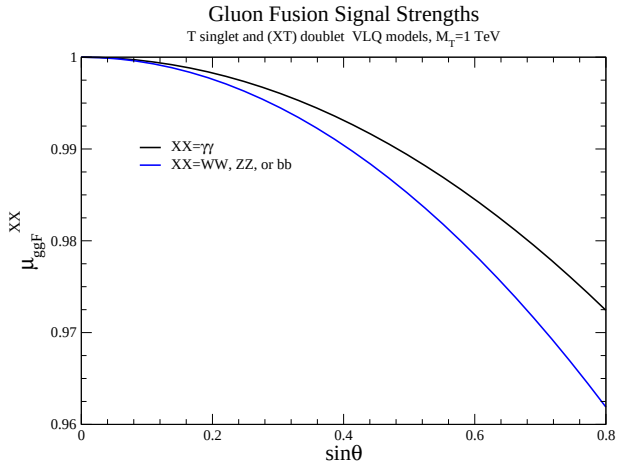


FIG. 11: Higgs branching ratios in VLQ models with a ($T$) singlet or an ($XT$) doublet normalized to the Standard Model predictions.

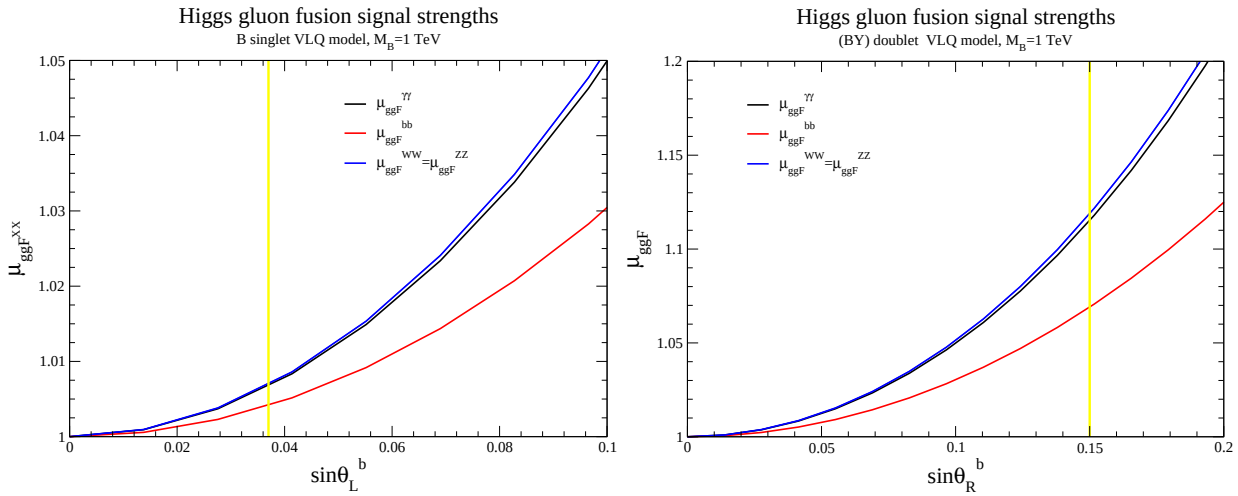


FIG. 12: Higgs branching ratios in VLQ models normalized to the SM predictions. The vertical yellow lines are the maximum mixing allowed by the electroweak fits for the $B$ singlet (LHS) and ($BY$) doublet (RHS) models shown in Fig. 7.

## V. CONCLUSIONS

We have considered restrictions on the parameters of models with vector-like quarks and updated electroweak fits to the parameters of these models. The constraints on VLQ masses and mixings are strengthened from previous fits. Mixing in the $B$ VLQ sector is highly constrained due to the tree-level effect on the $Zb\bar{b}$ coupling, while mixings up to $s_R^t \sim 0.2$ are allowed in the $T$ singlet case. In the doublet models mixings up to $s_R \sim 0.1 - 0.15$ are allowed, with an interesting region of $0.3 \lesssim s_R^t \lesssim 0.6$ in the ($XT$) doublet scenario and non-zero mixing allowed in both the top and bottom sectors in the ($TB$) doublet model. In the triplet models the mixing is somewhat more constrained, $s_L^t \lesssim 0.07$. Finally, we show that in order for Higgs coupling measurements to probe regions beyond those excluded by precision fits, measurements of a few % will be required.

### Acknowledgements

We would like to thank G. Panico for useful discussion. SD thanks B. Jaeger and the University of Tuebingen where this work was begun and Fermilab where it was finally completed for their hospitality. This work is supported by the U.S. Department of Energy under grant DE-SC0012704, by the Swiss National Science Foundation (SNF) under contracts 200021-165772 and 200021-160814, and by the Advanced ERC Grant Pert QCD. The work of C.-Y.C

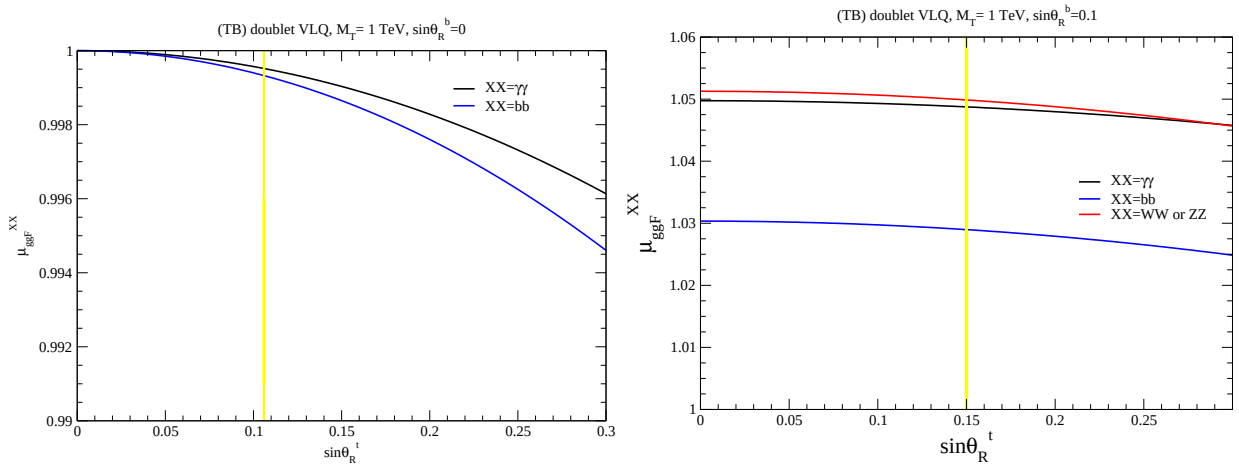


FIG. 13: Higgs gluon fusion signal strengths in $(TB)$ doublet VLQ model, normalized to the SM predictions. RHS has $s_R^b = 0.1$ and LHS has $s_R^b = 0$. The vertical yellow lines are the maximum mixing allowed by the electroweak fits of Fig. 9.

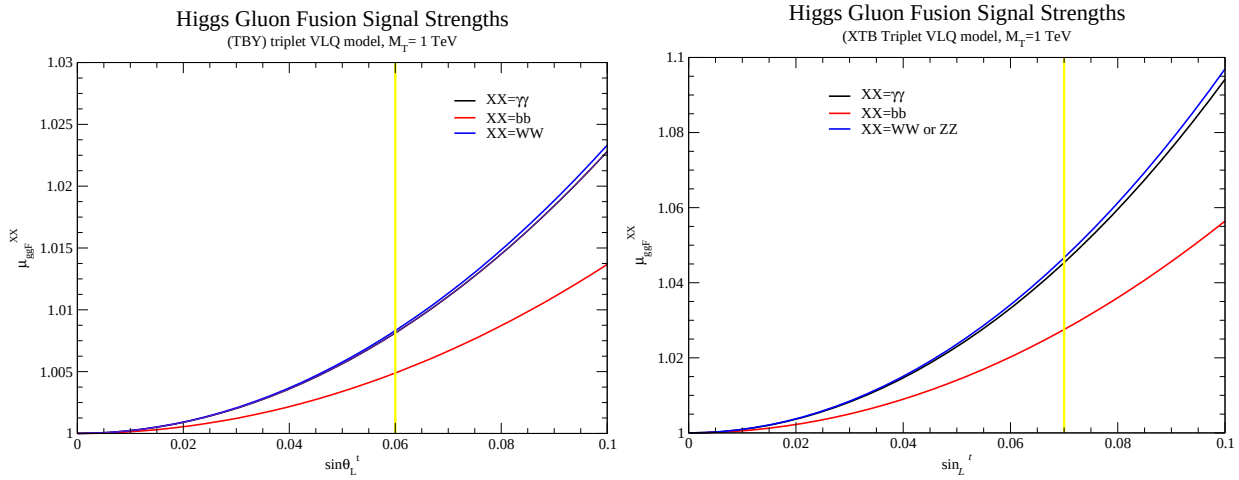


FIG. 14: Higgs branching ratios in the VLQ models normalized to the Standard Model predictions. The vertical yellow lines are the maximum mixing allowed by the electroweak fits for the $TBY$ triplet (LHS) and $(XTB)$ triplet (RHS) models shown in Fig. 7.

is supported by NSERC, Canada. Research at the Perimeter Institute is supported in part by the Government of Canada through NSERC and by the Province of Ontario through MEDT. Digital data related to our results can be found at `https://quark.phy.bnl.gov/Digital_Data_Archive/dawson/vlq_17/`

## Appendix A: VLQ Triplet Lagrangian

In the following, the fields are the current eigenstates, but for simplicity of notation we shall omit the superscript "0".
To establish our normalization convention, we shall use

$$\mathcal{L}^{(SM)} = \overline{\psi}_L \gamma^\mu i \left(\partial_\mu - igW_\mu(x) - ig' \mathbb{1}_{(2)} B_\mu(x)\right) \psi_L + \overline{q}_R \gamma^\mu i \left(\partial_\mu - ig' \mathbb{1}_{(1)} B_\mu(x)\right) q_R \ , \tag{A.1}$$

where $\psi_L$ is the top-bottom left-handed doublet, $q_R = \{t_R, b_R\}$ are the right-handed singlets, $W_\mu = W_\mu^a \frac{\sigma^a}{2}$ $(a = \{1,2,3\})$ and $\sigma^a$ are the Pauli matrices. They satisfy

$$\left[\sigma^a, \sigma^b\right] = 2i\epsilon^{abc}\sigma^c \qquad , \quad \mathrm{Tr}[\sigma^a \sigma^b] = 2\delta^{ab} \ . \tag{A.2}$$

The gauge boson interactions therefore read

$$\begin{aligned}\mathcal{L}^{(SM)}_{g.b.} &= eA_\mu \left[\bar{t}_{L,R}\gamma^\mu \left(\frac{I^{3(SM)}_{t_{L,R}}}{2} + Y^{(SM)}_{t_{L,R}}\right) t_{L,R} + \bar{b}_{L,R}\gamma^\mu \left(\frac{I^{3(SM)}_{b_{L,R}}}{2} + Y^{(SM)}_{b_{L,R}}\right) b_{L,R}\right] + \\ &\frac{g}{2c_W} Z_\mu \left[\bar{t}_{L,R}\gamma^\mu \left(I^{3(SM)}_{t_{L,R}} - 2Q^{(SM)}_t s^2_W\right) t_{L,R} + \bar{b}_{L,R}\gamma^\mu \left(I^{3(SM)}_{b_{L,R}} - 2Q^{(SM)}_b s^2_W\right) b_{L,R}\right] + \\ &\frac{g}{\sqrt{2}} W^+_\mu \bar{t}_L \gamma^\mu b_L + \frac{g}{\sqrt{2}} W^-_\mu \bar{b}_L \gamma^\mu t_L \ , \end{aligned} \tag{A.3}$$

where $I^{3(SM)}_q, Y^{(SM)}_q$ are the eigenvalues of the quark $q = \{t_{L,R}, b_{L,R}\}$ under $\sigma_3$ and the $U(1)_Y$ generator respectively,

$$\begin{aligned} &I^{3(SM)}_{t_R} = I^{3(SM)}_{b_R} = 0 \qquad\qquad , \quad I^{3(SM)}_{t_L} = -I^{3(SM)}_{b_R} = 1 \\ &Y^{(SM)}_{t_R} = \frac{2}{3} \quad , \quad Y^{(SM)}_{b_R} = -\frac{1}{3} \qquad , \quad Y^{(SM)}_{\psi_L} = \frac{1}{6} \ . \end{aligned} \tag{A.4}$$

This yields the correct charges for the top and bottom quarks (first line of eq. (A.3)). In the second line we replaced the hypercharge quantum number with the corresponding charge of the quark as derived from the first line.

As a reminder, the physical gauge bosons are defined by

$$W^\pm = \frac{W^1 \mp iW^2}{\sqrt{2}} \qquad , \quad W^3_\mu = c_W Z_\mu + s_W A_\mu \qquad , \quad B_\mu = c_W A_\mu - s_W Z_\mu \ , \tag{A.5}$$

and $e = g s_W = g' c_W$.

### 1. Vector Triplets

#### Introducing the fields

Let $\rho^0$ be a fermionic field that transforms as a triplet under $SU(2)_L$, i.e.[8]

$$\rho^0 \to U(x)\rho^0 U^{-1}(x) \qquad , \qquad U(x) = e^{i\alpha^a(x)\tau^a} \ . \tag{A.6}$$

Here $\alpha^a(x)$ are the gauge transformation parameters and $\tau^a = \frac{\sigma^a}{2}$. For simplicity of notation, from now on we will omit the subscript "0" in the fermionic fields and use $U \equiv U(x)$.
Note that we can decompose fermions in a $SU(2)_L$ triplet on the basis of Pauli matrices as

$$\rho = \rho^i \tau^i \qquad (W_\mu = W^i_\mu \tau^i) \ . \tag{A.7}$$

As for the charged gauge bosons, we introduce

$$\rho^\pm = \frac{\rho^1 \mp i\rho^2}{\sqrt{2}} \ , \tag{A.8}$$

and we can use that

$$\rho^1\tau^1 + \rho^2\tau^2 = \rho^+ \frac{\tau^1 + i\tau^2}{\sqrt{2}} + \rho^- \frac{\tau^1 - i\tau^2}{\sqrt{2}} \ . \tag{A.9}$$

Let us remind ourselves that the charges of $\tau^1 \pm i\tau^2$ (i.e. $\rho^\pm$ and $W^\pm$) are $\pm 1$ respectively,

$$[\tau^3, \tau^1 \pm i\tau^2] = \pm(\tau^1 \pm i\tau^2) \ . \tag{A.10}$$

---

[8] Recall that the triplet vector field $W_\mu$ transforms as

$$W_\mu \to U\left(W_\mu + \frac{i}{g}\partial_\mu\right) U^{-1} \ .$$

A triplet fermionic field has a similar transformation law, up to the shift term.

### Guage invariance and the Lagrangian

From the transformation laws of the gauge and fermion fields, the gauge-invariant covariant derivative must be defined as[9]

$$D_\mu \rho = \partial_\mu \rho - i\left[W_\mu, \rho\right] . \tag{A.11}$$

The Lagrangian, imposing also the correct normalization of the kinetic term and adding the $U(1)_Y$ part, is then

$$\begin{aligned}
\mathcal{L} &= 2\mathrm{Tr}\left\{\bar{\rho}\, i\gamma^\mu D_\mu\, \rho\right\} + 2\mathrm{Tr}\left\{g' Y \bar{\rho}\gamma^\mu B_\mu \rho\right\} \\
&= \frac{1}{2}\mathrm{Tr}\left\{\sigma^a\sigma^b\right\} i\bar{\rho}^a\gamma^\mu(\partial_\mu\rho^b) + \frac{1}{2}\mathrm{Tr}\left\{\sigma^a\left[\sigma^b,\sigma^c\right]\right\}\left(\frac{g}{2}\bar{\rho}^a\gamma^\mu W_\mu^c\rho^c\right) + \frac{1}{2}\mathrm{Tr}\left\{\sigma^a\sigma^b\right\}\left(g' Y\bar{\rho}^a\gamma^\mu B_\mu\rho^b\right) \\
&= \bar{\rho}^a\gamma^\mu(\partial_\mu\rho^a) + ig\bar{\rho}^a\gamma^\mu W_\mu^c\rho^c\epsilon^{abc} + g' Y\bar{\rho}^a\gamma^\mu B_\mu\rho^a .
\end{aligned} \tag{A.12}$$

### Couplings of the fermions to the EW gauge bosons

Let us recall that in the normalization we chose the $\{X,T,B\}$ triplet has isospin $I^3_{\rho_{XTB}} = \{2,0,-2\}$, $Y_{\rho_{XTB}} = \frac{2}{3}$, and the $\{T,B,Y\}$ triplet has $I^3_{\rho_{TBY}} = \{2,0,-2\}$, $Y_{\rho_{TBY}} = -\frac{1}{3}$. The couplings to the electroweak gauge bosons are easily derived from eq. (A.12) via the replacements

$$f^1 = \frac{f^+ + f^-}{\sqrt{2}} \qquad , \quad f^2 = i\frac{f^+ - f^-}{\sqrt{2}} \qquad , \quad f = \{\rho, W_\mu\} . \tag{A.13}$$

#### *Neutral couplings: the photon*

The photon couplings allow us to determine the electric charge of the three quarks. From the Lagrangian (A.12), with the definition of the gauge boson fields of the Standard Model, one gets

$$\mathcal{L}_\gamma = eA_\mu\left[\bar{\rho}^+\gamma^\mu\rho^+\left(Y + \frac{I^3_{\rho^+}}{2}\right) + \bar{\rho}^3\gamma^\mu\rho^3\,(Y) + \bar{\rho}^-\gamma^\mu\rho^-\left(Y + \frac{I^3_{\rho^-}}{2}\right)\right] . \tag{A.14}$$

Hence

- for the triplet of hypercharge $Y = \frac{2}{3}$, $\rho^+ \equiv X$ has charge 5/3, $\rho^3 \equiv T$ has charge 2/3, and $\rho^- \equiv B$ has charge -1/3;
- for the triplet of hypercharge $Y = -\frac{1}{3}$, $\rho^+ \equiv T$ has charge 2/3, $\rho^3 \equiv B$ has charge -1/3, and $\rho^- \equiv Y$ has charge -4/3,

as we expect.

#### *Neutral couplings: the Z boson*

The couplings of the quarks in the vector triplet to the $Z$ boson are

$$\begin{aligned}
\mathcal{L}_Z^{XTB} &= \frac{g}{2c_W}Z_\mu\left[\overline{X}\gamma^\mu X\left(I_q^3 - 2s_W^2 Q_X\right) + \overline{T}\gamma^\mu T\left(-2s_W^2 Q_T\right) + \overline{B}\gamma^\mu B\left(-I_3^q - 2s_W^2 Q_B\right)\right] \\
&= \frac{g}{2c_W}Z_\mu\left[\overline{X}\gamma^\mu X\left(2 - \frac{10}{3}s_W^2\right) + \overline{T}\gamma^\mu T\left(-\frac{4}{3}s_W^2\right) + \overline{B}\gamma^\mu B\left(-2 + \frac{2}{3}s_W^2\right)\right] ; \\
\mathcal{L}_Z^{TBY} &= \frac{g}{2c_W}Z_\mu\left[\overline{T}\gamma^\mu T\left(I_q^3 - 2s_W^2 Q_T\right) + \overline{B}\gamma^\mu B\left(-2s_W^2 Q_B\right) + \overline{Y}\gamma^\mu Y\left(-I_3^q - 2s_W^2 Q_Y\right)\right] \\
&= \frac{g}{2c_W}Z_\mu\left[\overline{T}\gamma^\mu T\left(2 - \frac{4}{3}s_W^2\right) + \overline{B}\gamma^\mu B\left(\frac{2}{3}s_W^2\right) + \overline{Y}\gamma^\mu T\left(-2 + \frac{8}{3}s_W^2\right)\right] .
\end{aligned} \tag{A.15}$$

---

[9] We want $D_\mu\rho \to U\,(D_\mu\rho)\,U^{-1}$, and we need to pick the same normalization conventions as those for the Standard Model.

This is perfectly consistent with what one expects from the Standard Model case (hypercharge minus twice the electric charge).

*Charged couplings*

The couplings to the charged gauge bosons are

$$\begin{aligned}\mathcal{L}_W^{XTB} &= gW_\mu^+\left(\overline{T}\gamma^\mu B - \overline{X}\gamma^\mu T\right) + gW_\mu^-\left(\overline{B}\gamma^\mu T - \overline{T}\gamma^\mu X\right) ,\\ \mathcal{L}_W^{TBY} &= gW_\mu^+\left(\overline{T}\gamma^\mu B - \overline{X}\gamma^\mu T\right) + gW_\mu^-\left(\overline{B}\gamma^\mu T - \overline{T}\gamma^\mu X\right)\end{aligned} \tag{A.16}$$

and similarly for the $Y = -\frac{1}{3}$ triplet. Notice that these couplings are a factor $\sqrt{2}$ larger than the Standard Model couplings (eq. (A.3)).

### 2. Physical couplings

To obtain the physical fields we follow the procedure described in eqs. (2.6 - 2.9)

$$Y = \tfrac{2}{3} \textit{ triplet } (X,T,B)$$

The physical couplings to the electroweak gauge bosons read (cfr. eqs. (A.3), (A.15), (A.16))

$$\begin{aligned}
X_{XX,L} &= \begin{pmatrix}2\end{pmatrix} & , \; X_{XX,R} &= \begin{pmatrix}2\end{pmatrix} & ,\\
X_{tt,L} &= \begin{pmatrix}(c_L^t)^2 & c_L^t s_L^t\\ c_L^t s_L^t & (s_L^t)^2\end{pmatrix} & , \; X_{tt,R} &= \begin{pmatrix}0 & 0\\ 0 & 0\end{pmatrix} & ,\\
X_{bb,L} &= \begin{pmatrix}-1-(s_L^b)^2 & c_L^b s_L^b\\ c_L^b s_L^b & -1-(c_L^b)^2\end{pmatrix} & , \; X_{bb,R} &= \begin{pmatrix}-2(s_R^b)^2 & 2c_R^b s_R^b\\ 2c_R^b s_R^b & -2(c_R^b)^2\end{pmatrix} & ,\\
A_{Xt,L} &= \begin{pmatrix}-\sqrt{2}s_L^t & \sqrt{2}c_L^t\end{pmatrix} & , \; A_{Xt,R} &= \begin{pmatrix}-\sqrt{2}s_R^t & \sqrt{2}c_R^t\end{pmatrix} & ,\\
A_{tb,L} &= \begin{pmatrix}c_L^b c_L^t + \sqrt{2}s_L^b s_L^t & c_L^t s_L^b - \sqrt{2}c_L^b s_L^t\\ c_L^b s_L^t - \sqrt{2}c_L^t s_L^b & s_L^b s_L^t + \sqrt{2}c_L^b c_L^t\end{pmatrix} & , \; A_{tb,R} &= \begin{pmatrix}\sqrt{2}s_R^b s_R^t & -\sqrt{2}c_R^b s_R^t\\ -\sqrt{2}c_R^t s_R^b & \sqrt{2}c_R^b c_R^t\end{pmatrix} & .
\end{aligned}$$

This is in agreement with the results of Ref. [19].

We also show here how one derives the relations among masses and angles of eq. (2.11) for the $(X,T,B)$ triplet. Starting from the Lagrangian (2.5), the bare mass matrices are

$$M^t = \begin{pmatrix}\lambda_t\frac{v}{\sqrt{2}} & \lambda_7\frac{v}{\sqrt{2}}\\ 0 & M_{XTB}\end{pmatrix} \quad , \quad M^b = \begin{pmatrix}\lambda_b\frac{v}{\sqrt{2}} & \lambda_7 v\\ 0 & M_{XTB}\end{pmatrix} . \tag{A.17}$$

Let us notice that

$$\left(M^q_{diag}\right)^2 = V_L^q M^q M^{q\dagger} V_L^{q,\dagger} = V_R^q M^{q\dagger} M^q V_R^{q\dagger} \qquad (q = t,b) . \tag{A.18}$$

The condition

$$\left(M^q_{diag}\right)^2_{(1,1)} = m_q^2$$

yields

$$\tan\theta_R^q = \frac{m_q}{M_Q}\tan\theta_L^q . \tag{A.19}$$

Next, one can "reconstruct" the square bare mass matrix, both in the top and bottom sector, inverting eq. (A.18). Imposing that the entry $(2,2)$ is the same and equals $M^2_{XTB} = M_X^2$, we get

$$M_X^2 = (c_{L,R}^b)^2 M_B^2 + (s_{L,R}^b)^2 m_b^2 = (c_{L,R}^t)^2 M_T^2 + (s_{L,R}^t)^2 m_t^2 . \tag{A.20}$$

Finally, using

$$V_L^{q\dagger}(M^q_{diag})^2 V_L^q = M^q M^{q\dagger} \qquad (q=t,b)\ , \tag{A.21}$$

and noticing that the entries $(1,2)$ of these matrices are related,

$$\left[M^b M^{b\dagger}\right]_{(1,2)} = \lambda_7 M_{XTB} = \sqrt{2}\left[M^t M^{t\dagger}\right]_{(1,2)} \tag{A.22}$$

yields

$$(M_B^2 - m_b^2)\sin 2\theta_L^b = \sqrt{2}(M_T^2 - m_t^2)\sin 2\theta_L^t\ . \tag{A.23}$$

$$Y = -\tfrac{1}{3}\ \textit{triplet}\ (T,B,Y)$$

The physical couplings to the electroweak gauge bosons read (cfr. eqs. (A.3), (A.15), (A.16))

$$\begin{aligned}
X_{tt,L} &= \begin{pmatrix} 1+(s_L^t)^2 & -c_L^t s_L^t \\ -c_L^t s_L^t & 1+(c_L^t)^2 \end{pmatrix} && , \ X_{tt,R} = \begin{pmatrix} 2(s_R^t)^2 & -2c_R^t s_R^t \\ -2c_R^t s_R^t & 2(c_R^t)^2 \end{pmatrix} , \\
X_{bb,L} &= \begin{pmatrix} -(c_L^b)^2 & -c_L^b s_L^b \\ -c_L^b s_L^b & -(s_L^b)^2 \end{pmatrix} && , \ X_{bb,R} = \begin{pmatrix} 0 & 0 \\ 0 & 0 \end{pmatrix} , \\
X_{YY,L} &= \begin{pmatrix} -2 \end{pmatrix} && , \ X_{YY,R} = \begin{pmatrix} -2 \end{pmatrix} , \\
A_{tb,L} &= \begin{pmatrix} c_L^b c_L^t + \sqrt{2}s_L^b s_L^t & c_L^t s_L^b - \sqrt{2}c_L^b s_L^t \\ c_L^b s_L^t - \sqrt{2}c_L^t s_L^b & s_L^b s_L^t + \sqrt{2}c_L^b c_L^t \end{pmatrix} && , \ A_{tb,R} = \begin{pmatrix} \sqrt{2}s_R^b s_R^t & -\sqrt{2}c_R^b s_R^t \\ -\sqrt{2}c_R^t s_R^b & \sqrt{2}c_R^b c_R^t \end{pmatrix} , \\
A_{bY,L} &= \begin{pmatrix} -\sqrt{2}s_L^b \\ \sqrt{2}c_L^b \end{pmatrix} && , \ A_{bY,R} = \begin{pmatrix} -\sqrt{2}s_R^b \\ \sqrt{2}c_R^b \end{pmatrix} .
\end{aligned}$$

The top and bottom mass matrices are (eq. (2.5))

$$M^t = \begin{pmatrix} \lambda_t \frac{v}{\sqrt{2}} & \lambda_8 v \\ 0 & M_{TBY} \end{pmatrix} \quad , \quad M^b = \begin{pmatrix} \lambda_b \frac{v}{\sqrt{2}} & \lambda_8 \frac{v}{\sqrt{2}} \\ 0 & M_{TBY} \end{pmatrix}\ . \tag{A.24}$$

Following the same proof that lead to eqs. (A.19) and (A.20), we obtain

$$\begin{aligned}
\tan\theta_R^q &= \frac{m_q}{M_Q}\tan\theta_L^q\ , \\
M_Y^2 &= (c_{L,R}^b)^2 M_B^2 + (s_{L,R}^b)^2 m_b^2 \\
&= (c_{L,R}^t)^2 M_T^2 + (s_{L,R}^t)^2 m_t^2\ .
\end{aligned} \tag{A.25}$$

Similarly, the equivalent of eq. (A.23) is

$$(M_T^2 - m_t^2)\sin 2\theta_L^t = \sqrt{2}(M_B^2 - m_b^2)\sin 2\theta_L^b\ . \tag{A.26}$$

### Appendix B: EFT Coefficients and limits from $b$ and Higgs Couplings

Searches for VLQs at the LHC suggest that the masses are relatively heavy, $M \gtrsim \mathcal{O}(800-1000)$ GeV [25–37]. This means that we are always in the regime,

$$\frac{m_t}{M} << 1, \quad \frac{m_b}{M} \sim 0, \tag{B.1}$$

where an effective field theory approach is warranted. The Lagrangian involving third generation SM quarks and VLQs can be written as,

$$L \ = \ L_{Y,SM} + L_{KE} + L_Q \tag{B.2}$$

where $L_{Y,SM}$ is defined in Eq. 2.3, $L_Q$ contains the VLQ interactions given in Eq. 2.5 and $L_{KE}$ is the kinetic energy term. At tree level, the heavy VLQs can be integrated out using the equations of motion [49–51], generating an effective low-energy Lagrangian that only contains SM fields,

$$L_{eff} = L_{Y,SM} + L'_{KE} + L_{qH} \tag{B.3}$$

| | $C_{Ht}$ | $C_{Hb}$ | $C_{Hq}$ | $C^s_{Hq}$ | $C^b_{HY}$ | $C^t_{HY}$ | $C_{Htb}$ |
|---|---|---|---|---|---|---|---|
| $T$ | 0 | 0 | $\frac{\lambda_1^2}{4M_T^2}$ | $-\frac{\lambda_1^2}{4M_T^2}$ | 0 | $\frac{\lambda_t\lambda_1^2}{2M_T^2}$ | 0 |
| $B$ | 0 | 0 | $-\frac{\lambda_2^2}{4M_B^2}$ | $-\frac{\lambda_2^2}{4M_B^2}$ | $\frac{\lambda_b\lambda_2^2}{2M_B^2}$ | 0 | 0 |
| $(T,B)$ | $-\frac{\lambda_4^2}{2M_T^2}$ | $\frac{\lambda_5^2}{2M_T^2}$ | 0 | 0 | $\frac{\lambda_b\lambda_5^2}{2M_T^2}$ | $\frac{\lambda_t\lambda_4^2}{2M_T^2}$ | $\frac{\lambda_4\lambda_5}{M_T^2}$ |
| $(X,T)$ | $\frac{\lambda_3^2}{2M_X^2}$ | 0 | 0 | 0 | 0 | $\frac{\lambda_t\lambda_3^2}{2M_X^2}$ | 0 |
| $(B,Y)$ | 0 | $-\frac{\lambda_6^2}{2M_B^2}$ | 0 | 0 | $\frac{\lambda_b\lambda_6^2}{2M_B^2}$ | 0 | 0 |
| $(X,T,B)$ | 0 | 0 | $\frac{3\lambda_7^2}{4M_T^2}$ | $\frac{\lambda_7^2}{4M_T^2}$ | $\frac{\lambda_7^2\lambda_b}{M_T^2}$ | $\frac{\lambda_7^2\lambda_t}{2M_T^2}$ | 0 |
| $(T,B,Y)$ | 0 | 0 | $-\frac{3\lambda_8^2}{4M_B^2}$ | $-\frac{\lambda_8^2}{4M_B^2}$ | $\frac{\lambda_8^2\lambda_b}{2M_B^2}$ | $\frac{\lambda_8^2\lambda_t}{M_B^2}$ | 0 |

TABLE IV: EFT coefficients for VLQ models in the large VLQ mass limit.

where $L'_{KE}$ now includes only the SM quarks and

$$L_{qH} = \Sigma_i C_i O_i + h.c. \tag{B.4}$$

contains the effective interactions of the SM quarks with the gauge and Higgs boson through higher dimensional operators (we restrict to dimension-6 operators). We have normalized the coefficients of these operators to be $\mathcal{O}\left(\frac{1}{M^2}\right)$. The new Higgs-fermion dimension-6 operators are [52]:

$$\begin{aligned}
O_{Ht} &= i(H^\dagger D_\mu H)(\overline{t}_R\gamma^\mu t_R) \\
O_{Hb} &= i(H^\dagger D_\mu H)(\overline{b}_R\gamma^\mu b_R) \\
O_{Hq} &= i(H^\dagger D_\mu H)(\overline{\psi}_L\gamma^\mu \psi_L) \\
O^s_{Hq} &= i(H^\dagger \sigma^a D_\mu H)(\overline{\psi}_L\sigma^a\gamma^\mu \psi_L) \\
O^b_{HY} &= (H^\dagger H)(\overline{\psi}_L H b_R) \\
O^t_{HY} &= (H^\dagger H)(\overline{\psi}_L \tilde{H} t_R) \\
O_{Htb} &= (\tilde{H}^\dagger i D_\mu H)(\overline{t}_R\gamma^\mu b_R)\,.
\end{aligned} \tag{B.5}$$

To $\mathcal{O}(\frac{1}{M^2})$, the coefficients of Eq. B.4 are given in Table IV in terms of the Yukawa couplings and we assume the splitting between the VLQ masses in a given representation are small, corresponding to small mixing angles. The different VLQ representations have quite different patterns for the coefficients [50, 52, 53].

These operators generate non-SM interactions of the fermions with the gauge and Higgs bosons. The interactions with the $W$ boson defined in Eq. 2.14 become in the EFT limit,

$$\begin{aligned}
A^L_{tb} &= 1 + v^2 C^s_{Hq} \\
A^R_{tb} &= \frac{v^2}{2} C_{Htb}\,,
\end{aligned} \tag{B.6}$$

and the couplings to the $Z$ boson defined in Eq. 2.15 are,

$$\begin{aligned}
\delta X^L_{tt} &= -\frac{v^2}{2}(C_{Hq} - C^s_{Hq}) \\
\delta X^R_{tt} &= -\frac{v^2}{2} C_{Ht} \\
\delta X^L_{bb} &= -\frac{v^2}{2}(C_{Hq} + C^s_{Hq}) \\
\delta X^R_{bb} &= -\frac{v^2}{2} C_{Hb}\,.
\end{aligned} \tag{B.7}$$

From Table IV, we see that right-handed $W$ couplings are only generated in the $(TB)$ model, while non-standard $W_L$ couplings arise in the singlet and triplet models. In a similar fashion, the doublet VLQ models have SM couplings of the $Z$ boson to the top and bottom quarks. Measuring the gauge boson fermion couplings puts strong constraints on the possible VLQ representations.

Finally, the $t, b$ couplings to the Higgs boson are also modified,

$$\begin{aligned} L_{Y,SM} &\rightarrow L_h \equiv -Y_f \overline{f} f h \\ Y_f &= \frac{1}{\sqrt{2}}\left(\lambda_f - \frac{3v^2}{2} C^f_{HY}\right), \end{aligned} \tag{B.8}$$

corresponding to,

$$\frac{m_f}{v} = Y_f + \frac{v^2}{\sqrt{2}} C^f_{HY}\,. \tag{B.9}$$

For the singlet and triplet models, we have the interesting relation between the $Zf\overline{f}$ couplings and the Higgs Yukawa coupling,

$$\lambda_f(\delta X^L_{ff} - 2I^f_3 \delta X^R_{ff}) = -\frac{v^2}{2} C^f_{HY} \quad \text{singlet, triplet VLQs}\,. \tag{B.10}$$

For non-zero $C^f_{HY}$, the Yukawa coupling is no longer proportional to the mass, leading to flavor non-diagonal Higgs-fermion interactions [54, 55].


[1] Charalampos Anastasiou, Stephan Buehler, Elisabetta Furlan, Franz Herzog, and Achilleas Lazopoulos. Higgs production cross-section in a Standard Model with four generations at the LHC. *Phys. Lett.*, B702:224–227, 2011.

[2] Charalampos Anastasiou, Claude Duhr, Falko Dulat, Elisabetta Furlan, Thomas Gehrmann, Franz Herzog, Achilleas Lazopoulos, and Bernhard Mistlberger. High precision determination of the gluon fusion Higgs boson cross-section at the LHC. *JHEP*, 05:058, 2016.

[3] Measurements of the Higgs boson production and decay rates and constraints on its couplings from a combined ATLAS and CMS analysis of the LHC pp collision data at $\sqrt{s} = 7$ and 8 TeV. Technical Report ATLAS-CONF-2015-044, CERN, Geneva, Sep 2015.

[4] Charalampos Anastasiou, Elisabetta Furlan, and Jose Santiago. Realistic Composite Higgs Models. *Phys. Rev.*, D79:075003, 2009.

[5] Roberto Contino. The Higgs as a Composite Nambu-Goldstone Boson. In *Physics of the large and the small, TASI 09, proceedings of the Theoretical Advanced Study Institute in Elementary Particle Physics, Boulder, Colorado, USA, 1-26 June 2009*, pages 235–306, 2011.

[6] Roberto Contino, Leandro Da Rold, and Alex Pomarol. Light custodians in natural composite Higgs models. *Phys. Rev.*, D75:055014, 2007.

[7] Kaustubh Agashe and Roberto Contino. The Minimal composite Higgs model and electroweak precision tests. *Nucl. Phys.*, B742:59–85, 2006.

[8] M. Gillioz, R. Grober, C. Grojean, M. Muhlleitner, and E. Salvioni. Higgs Low-Energy Theorem (and its corrections) in Composite Models. *JHEP*, 10:004, 2012.

[9] Giuliano Panico and Andrea Wulzer. The Composite Nambu-Goldstone Higgs. *Lect. Notes Phys.*, 913:pp.1–316, 2016.

[10] N. Arkani-Hamed, A. G. Cohen, E. Katz, and A. E. Nelson. The Littlest Higgs. *JHEP*, 07:034, 2002.

[11] Tao Han, Heather E. Logan, and Lian-Tao Wang. Smoking-gun signatures of little Higgs models. *JHEP*, 01:099, 2006.

[12] Jay Hubisz and Patrick Meade. Phenomenology of the littlest Higgs with T-parity. *Phys. Rev.*, D71:035016, 2005.

[13] L. Lavoura and Joao P. Silva. The Oblique corrections from vector - like singlet and doublet quarks. *Phys. Rev.*, D47:2046–2057, 1993.

[14] C. P. Burgess, Stephen Godfrey, Heinz Konig, David London, and Ivan Maksymyk. Model independent global constraints on new physics. *Phys. Rev.*, D49:6115–6147, 1994.

[15] F. del Aguila, J. A. Aguilar-Saavedra, and R. Miquel. Constraints on top couplings in models with exotic quarks. *Phys. Rev. Lett.*, 82:1628–1631, 1999.

[16] J. A. Aguilar-Saavedra. Effects of mixing with quark singlets. *Phys. Rev.*, D67:035003, 2003. [Erratum: Phys. Rev.D69,099901(2004)].

[17] Giacomo Cacciapaglia, Aldo Deandrea, Daisuke Harada, and Yasuhiro Okada. Bounds and Decays of New Heavy Vector-like Top Partners. *JHEP*, 11:159, 2010.

[18] S. Dawson and E. Furlan. A Higgs Conundrum with Vector Fermions. *Phys. Rev.*, D86:015021, 2012.

[19] J. A. Aguilar-Saavedra, R. Benbrik, S. Heinemeyer, and M. Prez-Victoria. Handbook of vectorlike quarks: Mixing and single production. *Phys. Rev.*, D88(9):094010, 2013.

[20] Sebastian A. R. Ellis, Rohini M. Godbole, Shrihari Gopalakrishna, and James D. Wells. Survey of vector-like fermion extensions of the Standard Model and their phenomenological implications. *JHEP*, 09:130, 2014.

[21] Andrei Angelescu, Abdelhak Djouadi, and Grgory Moreau. Vector-like top/bottom quark partners and Higgs physics at the LHC. *Eur. Phys. J.*, C76(2):99, 2016.

[22] Svjetlana Fajfer, Admir Greljo, Jernej F. Kamenik, and Ivana Mustac. Light Higgs and Vector-like Quarks without Prejudice. *JHEP*, 07:155, 2013.

[23] Ashutosh Kumar Alok, Subhashish Banerjee, Dinesh Kumar, S. Uma Sankar, and David London. New-physics signals of a model with a vector-singlet up-type quark. *Phys. Rev.*, D92:013002, 2015.

[24] Ashutosh Kumar Alok, Subhashish Banerjee, Dinesh Kumar, and S. Uma Sankar. Flavor signatures of isosinglet vector-like down quark model. *Nucl. Phys.*, B906:321–341, 2016.

[25] Search for pair production of vector-like top partners in events with exactly one lepton and large missing transverse momentum in $\sqrt{s} = 13$ TeV $pp$ collisions with the ATLAS detector. Technical Report ATLAS-CONF-2016-101, CERN, Geneva, Sep 2016.

[26] Search for pair production of heavy vector-like quarks decaying to high-$p_T$ $W$ bosons and b quarks in the lepton-plus-jets final state in pp collisions at $\sqrt{s}$=13 TeV with the ATLAS detector. Technical Report ATLAS-CONF-2016-102, CERN, Geneva, Sep 2016.

[27] Search for production of vector-like top quark pairs and of four top quarks in the lepton-plus-jets final state in $pp$ collisions at $\sqrt{s} = 13$ TeV with the ATLAS detector. Technical Report ATLAS-CONF-2016-013, CERN, Geneva, Mar 2016.

[28] Georges Aad et al. Search for single production of a vector-like quark via a heavy gluon in the $4b$ final state with the ATLAS detector in $pp$ collisions at $\sqrt{s} = 8$ TeV. *Phys. Lett.*, B758:249–268, 2016.

[29] Georges Aad et al. Search for single production of vector-like quarks decaying into Wb in pp collisions at $\sqrt{s} = 8$ TeV with the ATLAS detector. *Eur. Phys. J.*, C76(8):442, 2016.

[30] Georges Aad et al. Search for the production of single vector-like and excited quarks in the $Wt$ final state in $pp$ collisions at $\sqrt{s} = 8$ TeV with the ATLAS detector. *JHEP*, 02:110, 2016.

[31] Georges Aad et al. Search for production of vector-like quark pairs and of four top quarks in the lepton-plus-jets final state in $pp$ collisions at $\sqrt{s} = 8$ TeV with the ATLAS detector. *JHEP*, 08:105, 2015.

[32] Georges Aad et al. Search for vector-like $B$ quarks in events with one isolated lepton, missing transverse momentum and jets at $\sqrt{s} = 8$ TeV with the ATLAS detector. *Phys. Rev.*, D91(11):112011, 2015.

[33] Vardan Khachatryan et al. Search for pair-produced vector-like B quarks in proton-proton collisions at $\sqrt{s}$=8TeV. *Phys. Rev.*, D93(11):112009, 2016.

[34] Vardan Khachatryan et al. Search for vector-like T quarks decaying to top quarks and Higgs bosons in the all-hadronic channel using jet substructure. *JHEP*, 06:080, 2015.

[35] Serguei Chatrchyan et al. Search for top-quark partners with charge 5/3 in the same-sign dilepton final state. *Phys. Rev. Lett.*, 112(17):171801, 2014.

[36] Serguei Chatrchyan et al. Inclusive search for a vector-like T quark with charge $\frac{2}{3}$ in pp collisions at $\sqrt{s} = 8$ TeV. *Phys. Lett.*, B729:149–171, 2014.

[37] Search for pair production of vector-like top quarks in events with one lepton and an invisibly decaying $Z$ boson in $\sqrt{s} = 13$ TeV $pp$ collisions at the ATLAS detector. Technical Report ATLAS-CONF-2017-015, CERN, Geneva, Mar 2017.

[38] Search for single production of vector-like quarks decaying into $Wb$ in $pp$ collisions at $\sqrt{s} = 13$ TeV with the ATLAS detector. Technical Report ATLAS-CONF-2016-072, CERN, Geneva, Aug 2016.

[39] Giacomo Cacciapaglia, Aldo Deandrea, Naveen Gaur, Daisuke Harada, Yasuhiro Okada, and Luca Panizzi. Interplay of vector-like top partner multiplets in a realistic mixing set-up. *JHEP*, 09:012, 2015.

[40] Sally Dawson, Elisabetta Furlan, and Ian Lewis. Unravelling an extended quark sector through multiple Higgs production? *Phys. Rev.*, D87(1):014007, 2013.

[41] Mu-Chun Chen and Sally Dawson. One loop radiative corrections to the rho parameter in the littlest Higgs model. *Phys. Rev.*, D70:015003, 2004.

[42] C. Patrignani et al. Review of Particle Physics. *Chin. Phys.*, C40(10):100001, 2016.

[43] Marcela Carena, Eduardo Ponton, Jose Santiago, and C. E. M. Wagner. Electroweak constraints on warped models with custodial symmetry. *Phys. Rev.*, D76:035006, 2007.

[44] Jorge de Blas, Marco Ciuchini, Enrico Franco, Satoshi Mishima, Maurizio Pierini, Laura Reina, and Luca Silvestrini. Electroweak precision observables and Higgs-boson signal strengths in the Standard Model and beyond: present and future. 2016.

[45] M. Baak, J. Cth, J. Haller, A. Hoecker, R. Kogler, K. Mnig, M. Schott, and J. Stelzer. The global electroweak fit at NNLO and prospects for the LHC and ILC. *Eur. Phys. J.*, C74:3046, 2014.

[46] Marc Gillioz, Ramona Grber, Andreas Kapuvari, and Margarete Mhlleitner. Vector-like Bottom Quarks in Composite Higgs Models. *JHEP*, 03:037, 2014.

[47] Vardan Khachatryan et al. Measurement of the t-channel single-top-quark production cross section and of the $| V_{tb} |$ CKM matrix element in pp collisions at $\sqrt{s}$= 8 TeV. *JHEP*, 06:090, 2014.

[48] John F. Gunion, Howard E. Haber, Gordon L. Kane, and Sally Dawson. The Higgs Hunter's Guide. *Front. Phys.*, 80:1–404, 2000.

[49] J. A. Aguilar-Saavedra. A Minimal set of top-Higgs anomalous couplings. *Nucl. Phys.*, B821:215–227, 2009.

[50] Chien-Yi Chen, S. Dawson, and I. M. Lewis. Top Partners and Higgs Boson Production. *Phys. Rev.*, D90(3):035016, 2014.

[51] Cdric Delaunay, Christophe Grojean, and Gilad Perez. Modified Higgs Physics from Composite Light Flavors. *JHEP*, 09:090, 2013.

[52] F. del Aguila, M. Perez-Victoria, and Jose Santiago. Effective description of quark mixing. *Phys. Lett.*, B492:98–106, 2000.

[53] Brian Batell, Stefania Gori, and Lian-Tao Wang. Higgs Couplings and Precision Electroweak Data. *JHEP*, 01:139, 2013.

[54] Roni Harnik, Joachim Kopp, and Jure Zupan. Flavor Violating Higgs Decays. *JHEP*, 03:026, 2013.

[55] Wolfgang Altmannshofer, Stefania Gori, Alexander L. Kagan, Luca Silvestrini, and Jure Zupan. Uncovering Mass Gener-

ation Through Higgs Flavor Violation. *Phys. Rev.*, D93(3):031301, 2016.